

## Supporting Information

### Efficient Circularly Polarized Thermally Activated Delayed Fluorescence Hetero-[4]Helicene with Carbonyl-/ Sulfone-Bridged Triarylamine Structures

Sheng-Yi Yang<sup>1#</sup>, Qi-Sheng Tian<sup>1#</sup>, Xiang-Ji Liao<sup>2#</sup>, Zheng-Guang Wu<sup>2, 4</sup>, Wan-Shan Shen<sup>1</sup>, You-Jun Yu<sup>1</sup>, Zi-Qi Feng<sup>1</sup>, You-Xuan Zheng<sup>2\*</sup>, Zuo-Quan Jiang<sup>1\*</sup>, and Liang-Sheng Liao<sup>1, 3</sup>

<sup>1</sup> Institute of Functional Nano & Soft Materials (FUNSOM), Jiangsu Key Laboratory for Carbon-Based Functional Materials & Devices, Soochow University, Suzhou, Jiangsu 215123, China.

<sup>2</sup> State Key Laboratory of Coordination Chemistry, Jiangsu Key Laboratory of Advanced Organic Materials, School of Chemistry and Chemical Engineering, Nanjing University, Nanjing 210093, China.

<sup>3</sup> Macao Institute of Materials Science and Engineering, Macau University of Science and Technology, Macau 999078, China.

<sup>4</sup> Nantong Key Lab of Intelligent and New Energy Materials, College of Chemistry and Chemical Engineering, Nantong University, Nantong, 226019, China.

E-mail: yxzheng@nju.edu.cn; zqjiang@suda.edu.cn

#These authors contributed equally to this work.

## Contents

1	Experimental Section .....	S3
1.1	Materials and instruments .....	S3
1.2	Single crystal information .....	S5
1.3	Device fabrication process .....	S5
1.4	Syntheses of materials .....	S6
1.4.1	Synthesis of compound 2 .....	S6
1.4.2	Synthesis of compound 3 .....	S7
1.4.3	Synthesis of compound QPO .....	S8
1.4.4	Synthesis of compound 5 .....	S9
1.4.5	Synthesis of compound 6 .....	S10
1.4.6	Synthesis of compound QPO-Br .....	S10
1.4.7	Synthesis of compound QPO-PhCz .....	S11
1.5	Density functional theory .....	S12
2	Supplemental Figures .....	S18
2.1	Structural properties .....	S18
2.2	Photophysical properties .....	S19
2.3	Theoretical calculation .....	S20
2.4	Chiroptical properties .....	S21
2.5	Thermal properties .....	S29
2.6	Electrochemical properties .....	S30
2.7	Electroluminescence properties .....	S30
2.8	Circularly polarized electroluminescence properties .....	S32
3	Supplementary Tables .....	S33
3.1	Crystal data and structure refinement .....	S33
3.2	Electroluminescence characteristics .....	S35
4	Copy of NMR Spectra and MALDI-TOF-MS Plot .....	S36
4.1	$^1\text{H}$ NMR plot of 2, 400 MHz, $\text{CDCl}_3$ .....	S36
4.2	$^{13}\text{C}$ NMR plot of 2, 101 MHz, $\text{CDCl}_3$ .....	S36
4.3	$^1\text{H}$ NMR plot of 3, 400 MHz, $\text{CDCl}_3$ .....	S37
4.4	$^{13}\text{C}$ NMR plot of 3, 101 MHz, $\text{CDCl}_3$ .....	S37
4.5	$^1\text{H}$ NMR plot of QPO, 400 MHz, DMSO .....	S38
4.6	$^{13}\text{C}$ NMR plot of QPO, 101 MHz, DMSO .....	S38
4.7	$^1\text{H}$ NMR plot of 5, 400 MHz, $\text{CDCl}_3$ .....	S39
4.8	$^{13}\text{C}$ NMR plot of 5, 101 MHz, $\text{CDCl}_3$ .....	S39
4.9	$^1\text{H}$ NMR plot of 6, 400 MHz, $\text{CDCl}_3$ .....	S40
4.10	$^{13}\text{C}$ NMR plot of 6, 101 MHz, $\text{CDCl}_3$ .....	S40
4.11	$^1\text{H}$ NMR plot of QPO-Br, 400 MHz, DMSO .....	S41
4.12	$^{13}\text{C}$ NMR plot of QPO-Br, 101 MHz, DMSO .....	S41
4.13	$^1\text{H}$ NMR plot of QPO-PhCz, 400 MHz, $\text{CDCl}_3$ .....	S42
4.14	$^{13}\text{C}$ NMR plot of QPO-PhCz, 101 MHz, $\text{CDCl}_3$ .....	S42
4.15	MALDI-TOF-MS plot of QPO .....	S43
4.16	MALDI-TOF-MS plot of QPO-Br .....	S43
4.17	MALDI-TOF-MS plot of QPO-PhCz .....	S44
5	References .....	S44

# 1 Experimental Section

## 1.1 Materials and instruments

All chemicals and reagents were used as received from commercial sources without further purification. tetrahydrofuran and toluene used in synthetic routes were purified by PURE SOLV (Innovative Technology) purification system.  $^1\text{H}$  NMR and  $^{13}\text{C}$  NMR spectra were recorded on a Bruker 400 spectrometer or Bruker 600 spectrometer at room temperature. Mass spectroscopy was performed using a Thermo Fisher ISQ Single Quadrupole GC-MS with direct probe system. Matrix-assisted laser desorption/ionization time-of-flight mass spectrometry (MALDI-TOF-MS) was performed on Bruker Autoflex II/Compass 1.0. Elemental analysis was measured using Vario Micro cube. Ultra-violet-visible absorption spectra were measured by a Shimadzu UV-2600 spectrophotometer. Fluorescent and phosphorescent spectra were measured by a Hitachi F-4600 spectrophotometer. Thermogravimetric analysis (TGA) was performed by a METTLER TOLEDO TGA1 under nitrogen atmosphere. The temperature was increased to 700 °C with a heating rate of 10 °C/min. Differential scanning calorimetry (DSC) measurements were performed by a METTLER TOLEDO DSC1 under nitrogen atmosphere. The temperature was increased and decreased with a heating or cooling rate of 10 °C/min. Molecular geometries were extracted in single crystals and performed by Gaussian 09W program package with density functional theory (DFT) with Beck's three-parameter hybrid exchange functional<sup>[1, 2]</sup> and Lee, and Yang and Parr correlation functional<sup>[3]</sup> (B3LYP) with 6-31G(d) basic set. Non-covalent

interactions (NCI) of intramolecular interactions analyses were carried out by Multiwfn<sup>[4]</sup> with reduced density gradient (RDG).<sup>[5]</sup> The NCI results were plotted via VMD software (version 1.9.3).<sup>[6]</sup> Cyclic voltammetry (CV) was performed on a CHI 600D electrochemical work station with a scan rate of 100 mV S<sup>-1</sup> at room temperature under an argon flow, in which a Pt disk, a Pt plate and a Ag/AgCl electrode were used as working electrode, counter electrode and reference electrode in tetra-n-butylammonium hexa-fluorophosphates (*n*-Bu<sub>4</sub>NPF<sub>6</sub>, 0.1 M) dichloromethane/ *N,N*-dimethylformamide solution, respectively. For calibration, the redox potential of ferrocene/ferrocenium(Fc/Fc<sup>+</sup>) was measured under the same conditions. The photoluminescence quantum efficiency (PLQY) was measured using Hamamatsu C9920-02G in nitrogen or air atmosphere. Transient spectra were obtained by using Quantaurus-Tau fluorescence lifetime measurement system (C11367-03, Hamamatsu Photonics Co.) in air or nitrogen atmosphere. The separation of isomers with chiral configurations was performed by chiral high-performance liquid chromatography (HPLC) were separated by IG column which was employed as stationary phase and hexane/dichloromethane/isopropanol (70/20/10) as eluent. The circular dichroism (CD) spectra were measured on a Jasco-1500 circular dichroism spectrometer. The circularly polarized photoluminescence (CPPL) spectra were measured on a Jasco CPL-300 spectrophotometer with “Standard” sensitivity at 200 nm/min scan speed and respond time of 2.0 s employing “slit” mode. The circularly polarized electroluminescence (CPEL) spectra were measured on a JASCO CPPL-300 spectrophotometer with ‘Standard’ sensitivity at 200 nm/min scan speed and respond time of 2.0 s employing

“band” mode.

## 1.2 Single crystal information

A suitable crystal was selected and it on a 'Bruker APEX-II CCD' diffractometer. The crystal was kept at 100.0 or 173.0 K during data collection. Using Olex2, the structure was solved with the ShelXT structure solution program using Intrinsic Phasing and refined with the ShelXL refinement package using Least Squares minimization. The crystals of **QPO** and **QPO-PhCz** were grown by slow evaporation in CHCl<sub>2</sub> and methanol. The X-ray crystallographic coordinates for structure reported in this study have been deposited at the Cambridge Crystallographic Data Centre (CCDC), under deposition number **QPO** (2051469) and **QPO-PhCz** (2051470). These data can be obtained free of charge from The Cambridge Crystallographic Data Centre “[http://www.ccdc.cam.ac.uk/data\\_request/cif](http://www.ccdc.cam.ac.uk/data_request/cif)”.

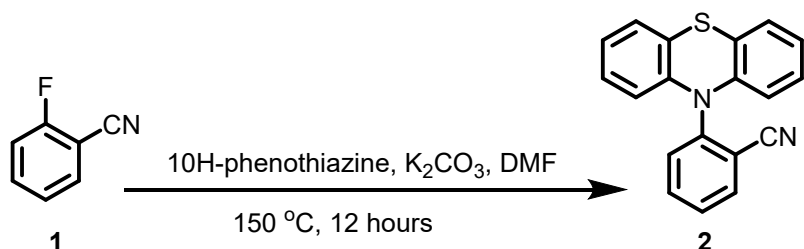
## 1.3 Device fabrication process

OLEDs were fabricated on ITO glass substrates layer (110 nm, 15 Ω/square) under a base pressure of  $3 \times 10^{-6}$  Torr. The active area of each device is 0.09 cm<sup>2</sup>. Deposition rates and thicknesses of all materials were monitored with oscillating quartz crystals. Doping layers were deposited by utilizing two different sensors to monitor the deposition rates of both host material and dopant material. The deposition rate of host was controlled at 0.2 nm s<sup>-1</sup>, and the deposition rate of the dopant was adjusted according to the volume ratio doped in the host materials. The electroluminescence

(EL) and current density-voltage(*J-V*) characteristics of the devices were measured by a constant current source (Keithley 2400 SourceMeter) combined with a photometer (Photo Research SpectraScan PR655).

## 1.4 Syntheses of materials

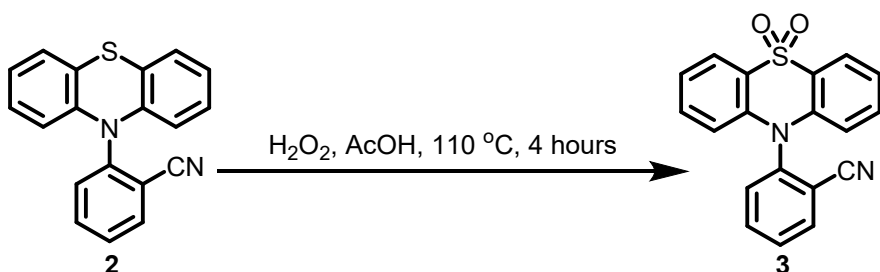
### 1.4.1 Synthesis of compound 2



A mixture of **1** (3.0 g, 24.79 mmol), 10H-phenothiazine (5.4 g, 27.27 mmol) and aqueous  $K_2CO_3$  (10.0 g, 74.37 mmol) in 100 mL *N,N*-Dimethylformamide (DMF) was stirred for 12 hours at  $150\text{ }^\circ C$  under a nitrogen atmosphere. After cooled to room temperature, the mixture was extracted with dichloromethane solution ( $4\times30$  mL), and the combined organic layer with dichloromethane (DCM) solution was dried over  $MgSO_4$ . We used rotary evaporation to remove off the solvent and used silica gel column to pass the residue, which using petroleum ether (PE)/ DCM (v/v, 4:1) as an eluent to obtain **2** as white solid (6.8 g, 92%).  $^1H$  NMR (400 MHz,  $CDCl_3$ )  $\delta$  7.93 (dd,  $J=7.7, 1.2$  Hz, 1H), 7.87 (td,  $J=7.9, 1.6$  Hz, 1H), 7.68 – 7.59 (m, 2H), 7.08 – 7.01 (m, 2H), 6.90 – 6.80 (m, 4H), 6.07 (dd,  $J=7.2, 2.2$  Hz, 2H).  $^{13}C$  NMR (101 MHz,  $CDCl_3$ )  $\delta$  143.7, 142.8, 135.3, 134.8, 133.5, 129.1, 127.1, 126.9, 123.2, 120.9, 116.2, 115.9, 115.3, 53.4. Anal. calcd for  $C_{19}H_{12}N_2S$  (%): C, 75.97; H, 4.03; N, 9.33; S, 10.67; found:

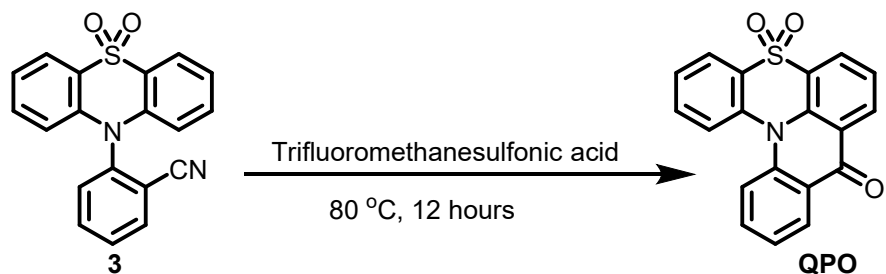
C, 75.84; H, 3.92; N, 9.25; S, 10.62.

#### 1.4.2 Synthesis of compound **3**



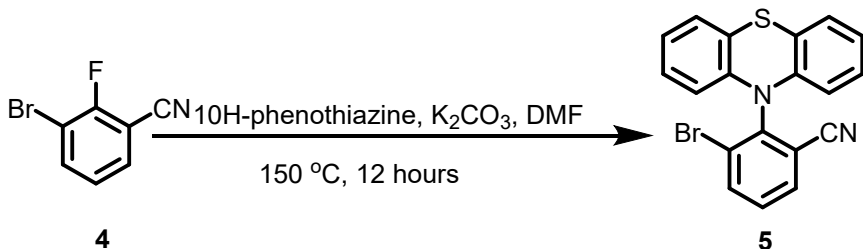
A mixture of **2** (3.0 g, 10.00 mmol) and  $\text{H}_2\text{O}_2$  (30 wt%, 10 mL) in 50 mL  $\text{CH}_3\text{COOH}$  was stirred for 4 hours at  $110^\circ\text{C}$  under an air atmosphere. After cooled to room temperature, the reaction system was extracted with dichloromethane ( $4 \times 45$  mL), and the combined organic solution was dried over  $\text{MgSO}_4$ . We used rotary evaporation to remove off the solvent and used silica gel column to pass the residue, which using PE/DCM (v/v, 3:1) as an eluent to obtain **3** as white solid (3.1 g, 95%).  $^1\text{H}$  NMR (400 MHz,  $\text{CDCl}_3$ )  $\delta$  8.21 (dd,  $J = 7.9, 1.5$  Hz, 2H), 8.03 (dd,  $J = 7.7, 1.4$  Hz, 1H), 7.96 (td,  $J = 7.8, 1.5$  Hz, 1H), 7.78 (td,  $J = 7.7, 1.1$  Hz, 1H), 7.63 – 7.53 (m, 1H), 7.45 (ddd,  $J = 8.7, 7.3, 1.6$  Hz, 2H), 7.36 – 7.28 (m, 2H), 6.47 (d,  $J = 8.5$  Hz, 2H).  $^{13}\text{C}$  NMR (101 MHz,  $\text{CDCl}_3$ )  $\delta$  141.3, 139.7, 136.1, 135.2, 133.2, 132.2, 130.6, 123.9, 123.5, 123.0, 116.3, 115.8, 114.9. Anal. calcd for  $\text{C}_{19}\text{H}_{12}\text{N}_2\text{O}_2\text{S}$  (%): C, 68.66; H, 3.64; N, 8.43; S, 9.65; found: C, 68.63; H, 3.70; N, 8.41; S, 9.76.

### 1.4.3 Synthesis of compound QPO



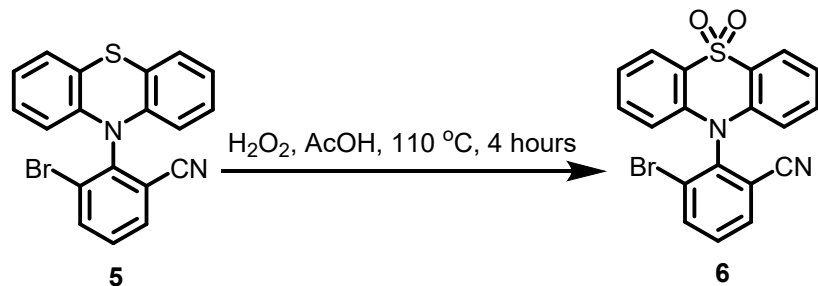
A mixture of **3** (3.0 g, 9.04 mmol) and trifluoromethanesulfonic acid (10 mL) in 50 mL single neck round bottom flask was stirred for 12 hours at 80 °C under an air atmosphere. After cooling to room temperature, the mixture was poured into 100 mL ice water and filtered to get crude product. The crude product was purified by column chromatography on silica gel using PE/ DCM (3/2, v/v) as eluent to afford **QPO** as yellow powder (1.1 g, 35%). <sup>1</sup>H NMR (400 MHz, DMSO-*d*<sub>6</sub>) δ 8.56 (dd, *J* = 7.8, 1.5 Hz, 1H), 8.45 (dd, *J* = 7.6, 1.5 Hz, 1H), 8.31 (dd, *J* = 7.9, 1.5 Hz, 1H), 8.19 (dd, *J* = 7.8, 1.5 Hz, 1H), 8.01 (d, *J* = 8.5 Hz, 1H), 7.91 – 7.81 (m, 2H), 7.80 – 7.71 (m, 2H), 7.68 – 7.53 (m, 2H). <sup>13</sup>C NMR (101 MHz, DMSO-*d*<sub>6</sub>) δ 177.4, 140.2, 139.6, 138.6, 134.5, 133.9, 131.9, 129.2, 128.6, 127.3, 127.1, 126.7, 126.2, 126.1, 125.0, 124.5, 124.2, 123.2, 121.8. MALDI-MS (m/z) of C<sub>19</sub>H<sub>11</sub>NO<sub>3</sub>S for [M+H]<sup>+</sup>: calcd. 333.05; found, 334.01. Anal. calcd for C<sub>19</sub>H<sub>11</sub>NO<sub>3</sub>S (%): C, 68.46; H, 3.33; N, 4.20; S, 9.62; found: C, 68.45; H, 3.33; N, 4.31; S, 9.83.

#### 1.4.4 Synthesis of compound 5



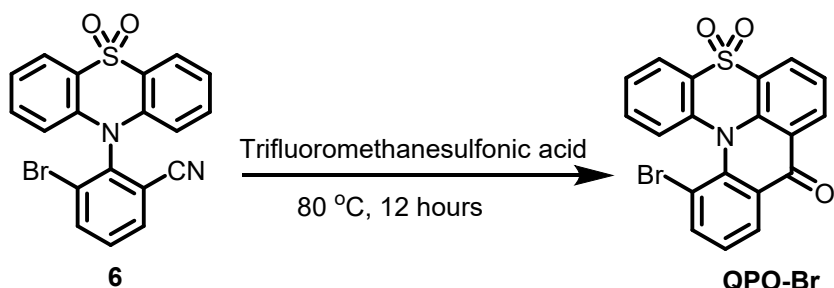
A mixture of **4** (5.0 g, 25.13 mmol), 10*H*-phenothiazine (5.5 g, 27.64 mmol) and aqueous  $\text{K}_2\text{CO}_3$  (17.3 g, 125.65 mmol) in 100 mL DMF was stirred for 12 hours at 150  $^\circ\text{C}$  under a nitrogen atmosphere. After cooled to room temperature, the mixture was extracted with dichloromethane solution (4×30 mL), and the combined organic layer with DCM solution was dried over  $\text{MgSO}_4$ . We used rotary evaporation to remove off the solvent and used silica gel column to pass the residue, which using PE/ DCM (v/v, 1:1) as an eluent to obtain **5** as white solid (8.5 g, 90%).  $^1\text{H}$  NMR (400 MHz,  $\text{CDCl}_3$ )  $\delta$  8.08 (dd,  $J = 8.2, 1.3$  Hz, 1H), 7.87 (dd,  $J = 7.7, 1.2$  Hz, 1H), 7.49 (t,  $J = 8.0$  Hz, 1H), 7.05 – 6.96 (m, 2H), 6.89 – 6.80 (m, 4H), 5.98 – 5.85 (m, 2H).  $^{13}\text{C}$  NMR (101 MHz,  $\text{CDCl}_3$ )  $\delta$  142.3, 140.2, 139.3, 134.1, 130.4, 128.5, 127.0, 126.9, 123.4, 120.2, 118.7, 115.3, 114.8. Anal. calcd for  $\text{C}_{19}\text{H}_{11}\text{BrN}_2\text{S}$  (%): C, 60.17; H, 2.92; N, 7.39; S, 8.45; found: C, 60.20; H, 2.96; N, 7.46; S, 8.81.

#### 1.4.5 Synthesis of compound **6**



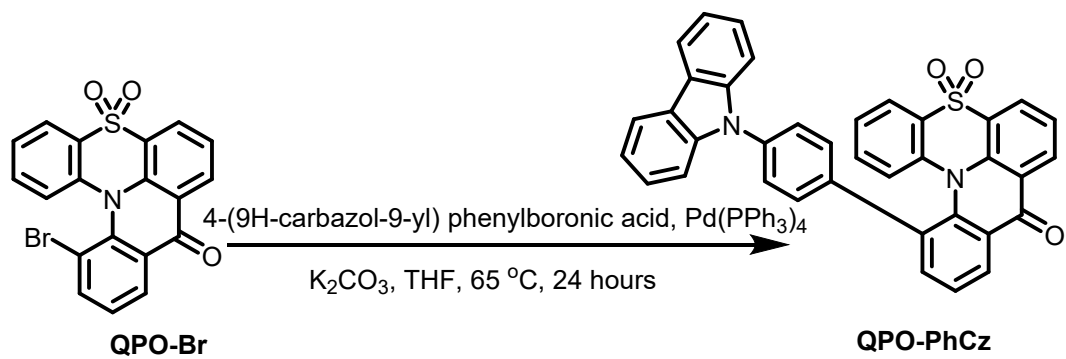
A mixture of **5** (5.0 g, 13.23 mmol) and  $\text{H}_2\text{O}_2$  (30 wt%, 20 mL) in 100 mL  $\text{CH}_3\text{COOH}$  was stirred for 4 hours at 110 °C under an air atmosphere. After cooled to room temperature, the reaction system was extracted with dichloromethane ( $4 \times 45$  mL), and the combined organic solution was dried over  $\text{MgSO}_4$ . We used rotary evaporation to remove off the solvent and used silica gel column to pass the residue, which using PE/DCM (v/v, 1:1) as an eluent to obtain **6** as white solid (4.9 g, 91%).  $^1\text{H}$  NMR (400 MHz,  $\text{CDCl}_3$ )  $\delta$  8.24 (dd,  $J = 7.9, 1.5$  Hz, 2H), 8.20 – 8.14 (m, 1H), 8.01 – 7.93 (m, 1H), 7.65 (t,  $J = 8.0$  Hz, 1H), 7.48 (ddd,  $J = 8.7, 7.3, 1.6$  Hz, 2H), 7.35 (t,  $J = 7.6$  Hz, 2H), 6.45 – 6.33 (m, 2H).  $^{13}\text{C}$  NMR (101 MHz,  $\text{CDCl}_3$ )  $\delta$  139.8, 139.7, 137.9, 134.1, 133.4, 131.7, 127.4, 124.3, 123.8, 123.3, 117.8, 115.4, 114.2. Anal. calcd for  $\text{C}_{19}\text{H}_{11}\text{BrN}_2\text{O}_2\text{S}$  (%): C, 55.49; H, 2.70; N, 6.81; S, 7.80; found: C, 55.60; H, 2.74; N, 6.83; S, 7.86.

#### 1.4.6 Synthesis of compound QPO-Br



A mixture of **6** (3.0 g, 7.32 mmol) and trifluoromethanesulfonic acid (15 mL) in 100 mL single neck round bottom flask was stirred for 12 hours at 80 °C under an air atmosphere. After cooling to room temperature, the mixture was poured into 150 mL ice water and filtered to get crude product. The crude product was purified by column chromatography on silica gel using PE/ DCM (1/1, v/v) as eluent to afford **QPO-Br** as yellow powder (0.9 g, 30%). <sup>1</sup>H NMR (400 MHz, DMSO-*d*<sub>6</sub>) δ 8.47 (ddd, *J* = 11.2, 7.7, 1.5 Hz, 2H), 8.36 (dd, *J* = 7.8, 1.5 Hz, 1H), 8.19 (dd, *J* = 7.8, 1.5 Hz, 1H), 8.12 (dd, *J* = 7.8, 1.5 Hz, 1H), 7.80 (t, *J* = 7.7 Hz, 1H), 7.67 (td, *J* = 8.5, 8.0, 1.6 Hz, 1H), 7.64 – 7.54 (m, 2H), 7.27 (d, *J* = 7.9 Hz, 1H). <sup>13</sup>C NMR (101 MHz, DMSO-*d*<sub>6</sub>) δ 177.6, 140.9, 140.6, 140.3, 138.9, 133.4, 131.7, 130.2, 129.1, 128.5, 128.2, 128.0, 127.0, 126.6, 125.6, 124.9, 123.9, 122.9, 116.3. MALDI-MS (m/z) of C<sub>19</sub>H<sub>10</sub>BrNO<sub>3</sub>S for [M+H]<sup>+</sup>: calcd. 410.96; found, 413.13. Anal. calcd for C<sub>19</sub>H<sub>10</sub>BrNO<sub>3</sub>S (%): C, 55.36; H, 2.45; N, 3.40; S, 7.78; found: C, 55.40; H, 2.51; N, 3.42; S, 7.72.

#### 1.4.7 Synthesis of compound **QPO-PhCz**



A mixture of **QPO-Br** (0.9 g, 2.19 mmol), 4-(9H-carbazol-9-yl) phenylboronic acid (0.8 g, 2.63 mmol), aqueous K<sub>2</sub>CO<sub>3</sub> (2.0 M, 5 mL) and Pd(PPh<sub>3</sub>)<sub>4</sub> (0.1 g, 0.11 mmol) in 100 mL tetrahydrofuran (THF) was stirred for 24 hours at 65 °C under a nitrogen

atmosphere. After cooled to room temperature, the mixture was extracted with dichloromethane solution ( $4 \times 30$  mL), and the combined organic layer with dichloromethane solution was dried over  $\text{MgSO}_4$ . We used rotary evaporation to remove off the solvent and used silica gel column to pass the residue, which using PE/DCM (v/v, 1:1) as an eluent to obtain **QPO-PhCz** as yellow solid (0.8 g, 61%).  $^1\text{H}$  NMR (400 MHz,  $\text{CDCl}_3$ )  $\delta$  8.73 – 8.63 (m, 1H), 8.62 – 8.54 (m, 1H), 8.43 (d,  $J = 7.5$  Hz, 1H), 8.13 (d,  $J = 7.7$  Hz, 2H), 7.93 (d,  $J = 6.0$  Hz, 2H), 7.77 – 7.60 (m, 4H), 7.43 (t,  $J = 6.8$  Hz, 4H), 7.30 (d,  $J = 7.5$  Hz, 2H), 7.24 – 7.11 (m, 4H), 7.10 – 7.02 (m, 1H).  $^{13}\text{C}$  NMR (101 MHz,  $\text{CDCl}_3$ )  $\delta$  178.5, 140.6, 137.7, 137.3, 137.1, 134.4, 131.9, 131.8, 128.8, 127.4, 126.5, 125.9, 125.5, 124.8, 124.2, 123.4, 121.9, 120.4, 120.1, 109.7. MALDI-MS (m/z) of  $\text{C}_{37}\text{H}_{22}\text{N}_2\text{O}_3\text{S}$  for  $[\text{M}+\text{H}]^+$ : calcd. 574.14; found, 574.09. Anal. calcd for  $\text{C}_{37}\text{H}_{22}\text{N}_2\text{O}_3\text{S}$  (%): C, 77.33; H, 3.86; N, 4.87; S, 5.58; found: C, 77.26; H, 3.82; N, 4.95; S, 5.61.

## 1.5 Density functional theory

The structural optimization of **QPO** and **QPO-PhCz** were conducted with the geometries obtained from the X-ray crystallographic analyses. The ground state moments of **QPO** and **QPO-PhCz** were obtained using density functional theory (DFT) method by adopting B3LYP/6-31g(d) level of theory.

Cartesian coordinates of **QPO** in ground state:

S	-2.43087400	0.55504700	0.76250300
O	-3.72384800	1.06250200	0.39908500

O	-2.17333900	0.31417800	2.15803500
O	3.41235800	2.00352100	-1.11385100
N	0.30911100	-0.35570700	0.05034300
C	-2.07413700	-0.90571300	-0.12138200
C	-1.17049900	1.58510800	0.12331700
C	-3.11024400	-1.72728500	-0.56154200
H	-4.01365800	-1.46145300	-0.43450800
C	-0.73270900	-1.24782700	-0.32589800
C	2.72213000	-0.00379600	-0.06376400
C	-1.41028300	2.93184500	-0.08764400
H	-2.28600400	3.28345900	0.02547700
C	0.09886800	1.02041100	-0.06392600
C	-0.45736600	-2.44580000	-0.99634300
H	0.44200900	-2.69058800	-1.17892400
C	-0.36819300	3.76937200	-0.46480200
H	-0.52557700	4.69293800	-0.62188100
C	1.85434200	-2.06494300	0.86142200
H	1.11998700	-2.62282900	1.08892500
C	-1.49155000	-3.27442000	-1.39289300
H	-1.28880100	-4.09840800	-1.81969800
C	2.51981700	1.34727400	-0.59923800
C	-2.82454800	-2.92675300	-1.18055600

H	-3.52480500	-3.50553300	-1.45769100
C	4.02167800	-0.46371700	0.18967400
H	4.76393600	0.07886300	-0.04810100
C	1.15703900	1.88227000	-0.41739300
C	1.62941900	-0.81875200	0.26484800
C	4.23952000	-1.68720300	0.77815900
H	5.12398200	-1.98794600	0.95061200
C	0.90080400	3.24190200	-0.60923600
H	1.61751800	3.81917500	-0.84494000
C	3.14438600	-2.48144700	1.11853000
H	3.28942400	-3.32324900	1.53413800

Cartesian coordinates of **QPO-PhCz** in ground state:

S	1.92428300	-2.52130300	-0.48825500
O	1.36334500	-2.04715200	-1.71936100
O	1.87828200	-3.92960300	-0.21526400
O	6.41540300	1.84889700	0.01080800
N	2.65871500	0.25509500	0.12632000
N	-3.63487300	0.38639300	-0.34253600
C	1.66190000	-0.28961500	0.99744500
C	3.75351800	-0.56777600	-0.17296900
C	2.79056800	1.66189700	-0.04911300

C	3.57143400	-1.94088200	-0.35319700
C	-5.33273100	-1.13587900	-0.22170400
C	5.06000800	-0.06037700	-0.23219400
C	1.24215800	-1.61569500	0.83042200
C	1.13616400	0.43925300	2.05843600
H	1.42823800	1.32951200	2.21359100
C	-4.83014400	1.10365300	-0.26113400
C	1.66203600	2.48671300	-0.21222400
C	-0.71883200	2.48772100	0.51769300
H	-0.50980600	3.21357700	1.09324400
C	-0.07719000	0.94715900	-1.20489200
H	0.58245400	0.58601900	-1.78580400
C	0.26835400	1.96647200	-0.31567500
C	-2.00117300	1.96626400	0.51936000
H	-2.65354400	2.30442400	1.12127100
C	-1.36880400	0.45800400	-1.24608700
H	-1.60367200	-0.21024900	-1.87917700
C	-3.93140200	-0.98184500	-0.30616100
C	4.08093100	2.22654200	-0.09631100
C	-2.32883500	0.94574100	-0.36061400
C	-5.89728700	0.19375900	-0.18412100
C	6.12738800	-0.94142400	-0.38593100

H	7.01025700	-0.59362000	-0.43344400
C	-5.87865000	-2.41375600	-0.17370100
H	-6.82059900	-2.53454400	-0.14669900
C	0.19029400	-0.13071400	2.88567100
H	-0.18237500	0.38417800	3.59149900
C	0.31487200	-2.19440900	1.69062200
H	0.05698600	-3.10162100	1.57809600
C	-3.07363000	-2.07665600	-0.27657400
H	-2.13111200	-1.96569500	-0.30614900
C	5.28520800	1.38439500	-0.07980600
C	-7.21035700	0.66966300	-0.10960100
H	-7.94333300	0.06751900	-0.05504800
C	4.63997700	-2.80483200	-0.47206000
H	4.48929400	-3.73924600	-0.55514500
C	1.85977300	3.85910500	-0.29492800
H	1.10324300	4.42913800	-0.36180900
C	-7.41823900	2.03406100	-0.11876500
H	-8.30339400	2.37237700	-0.05286300
C	5.94089000	-2.30676800	-0.47084800
H	6.68451000	-2.89461600	-0.52793900
C	-3.64547100	-3.32983100	-0.20197800
H	-3.08256500	-4.09474300	-0.17374000

C	-5.03675200	-3.50246800	-0.16590400
H	-5.40171400	-4.37876400	-0.13574700
C	-0.22467400	-1.43756700	2.70698200
H	-0.87988100	-1.81299300	3.28335100
C	-5.04375300	2.47871600	-0.29550900
H	-4.31932900	3.08871100	-0.36606600
C	-6.35179700	2.92218100	-0.22039500
H	-6.52656500	3.85604600	-0.24093200
C	4.22741900	3.60925100	-0.20743100
H	5.09852900	3.98829300	-0.23145400
C	3.13246100	4.42511900	-0.28149700
H	3.23891800	5.36855100	-0.32472800

## 2 Supplemental Figures

### 2.1 Structural properties

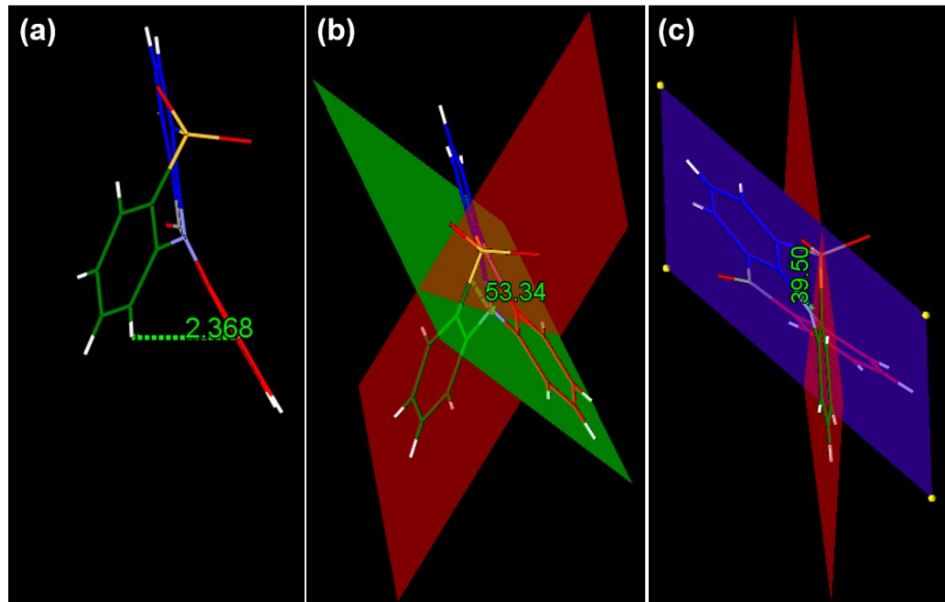


**Figure S1.** The details structure of QPO.

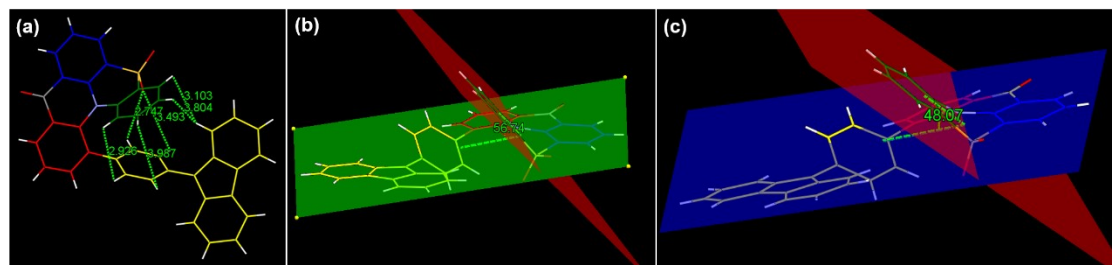


**Figure S2.** The details structure of QPO-PhCz.

## 2.2 Photophysical properties

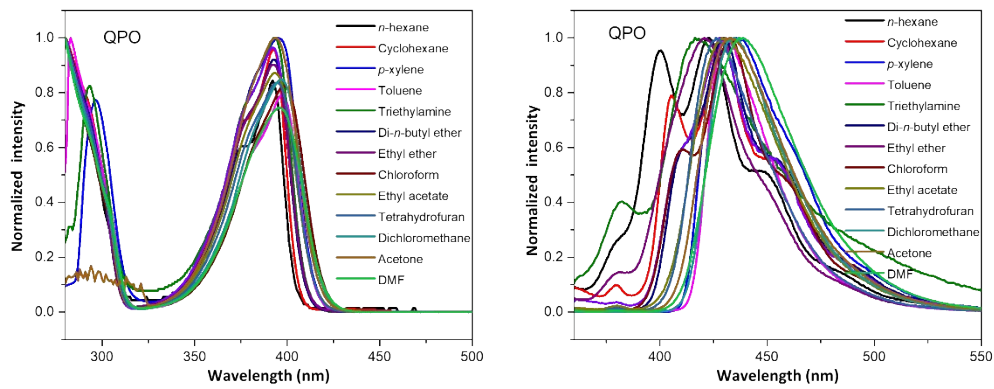


**Figure S3.** Solvent effect on the ultraviolet–visible absorption spectra and photoluminescence spectra of **QPO**.

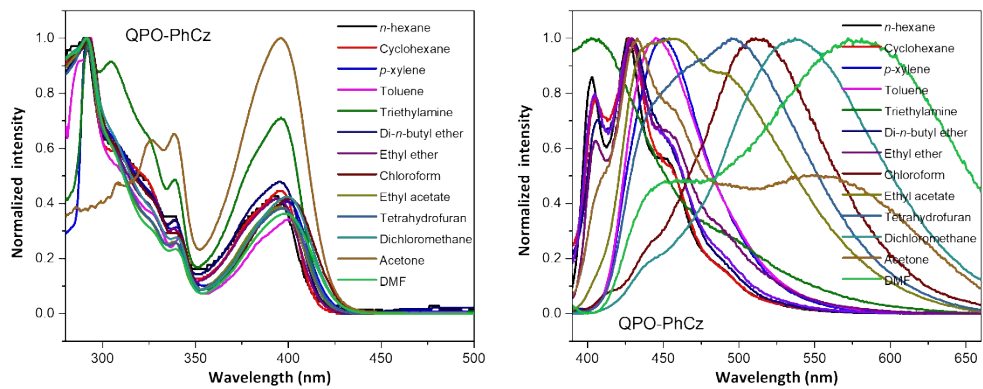


**Figure S4.** Solvent effect on the ultraviolet–visible absorption spectra and photoluminescence spectra of **QPO-PhCz**.

## 2.3 Theoretical calculation

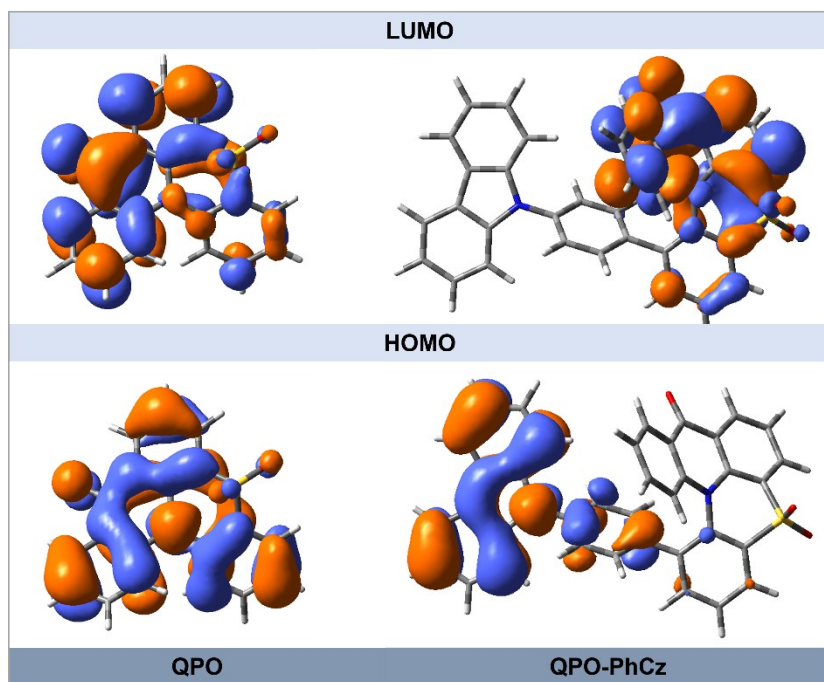
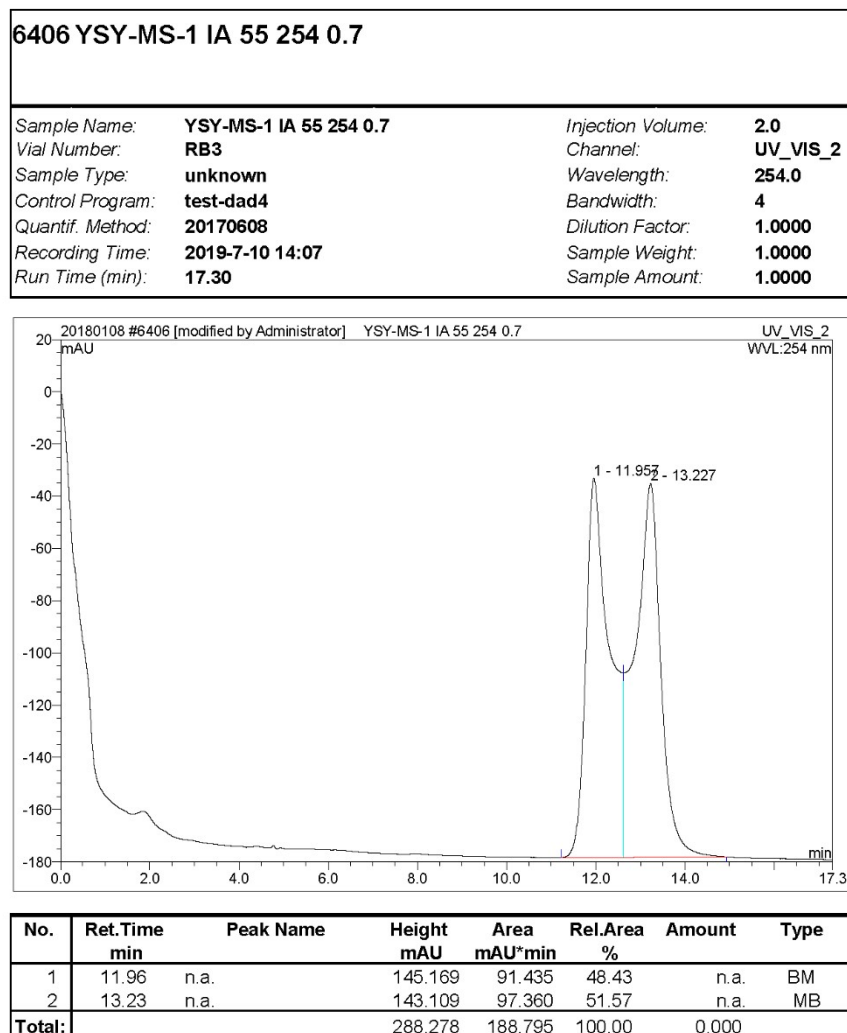


**Figure S5.** HOMO and LUMO orbital distributions based on DFT at the B3LYP functional and 6-31G(d) basis set.

## 2.4 Chiroptical properties

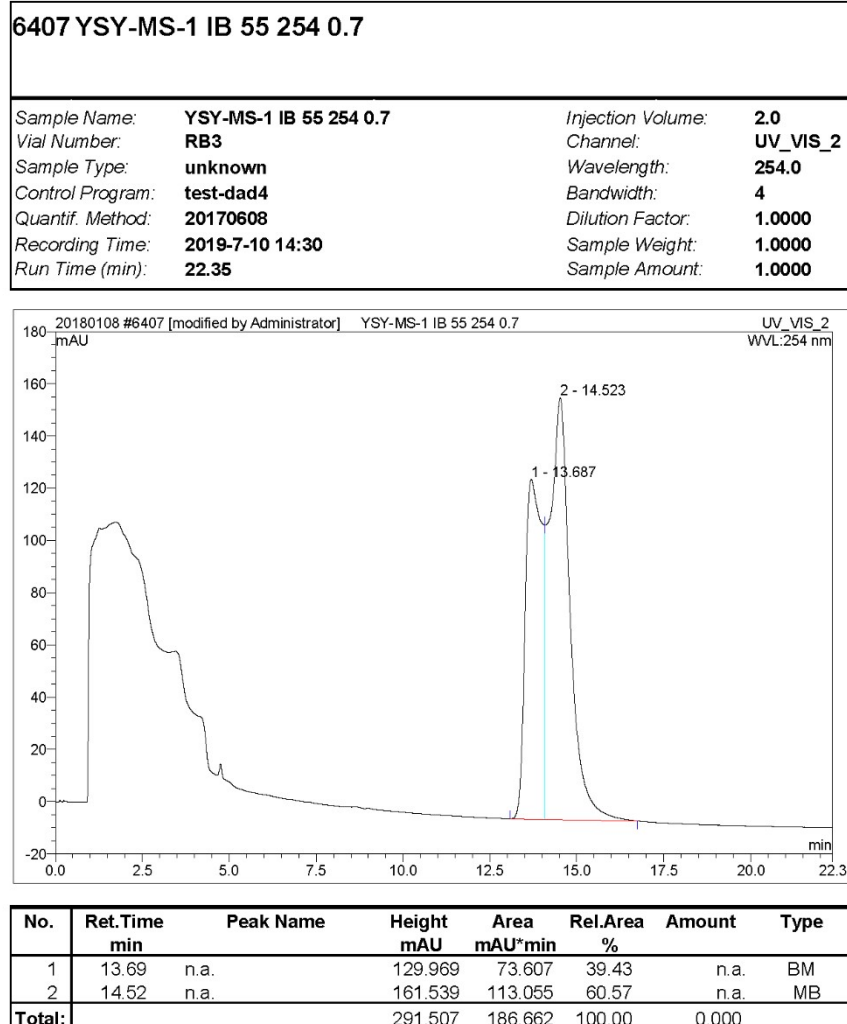
Operator:Administrator Timebase:HPLC Sequence:20180108

Page 1-1  
2019-7-10 2:45 下午



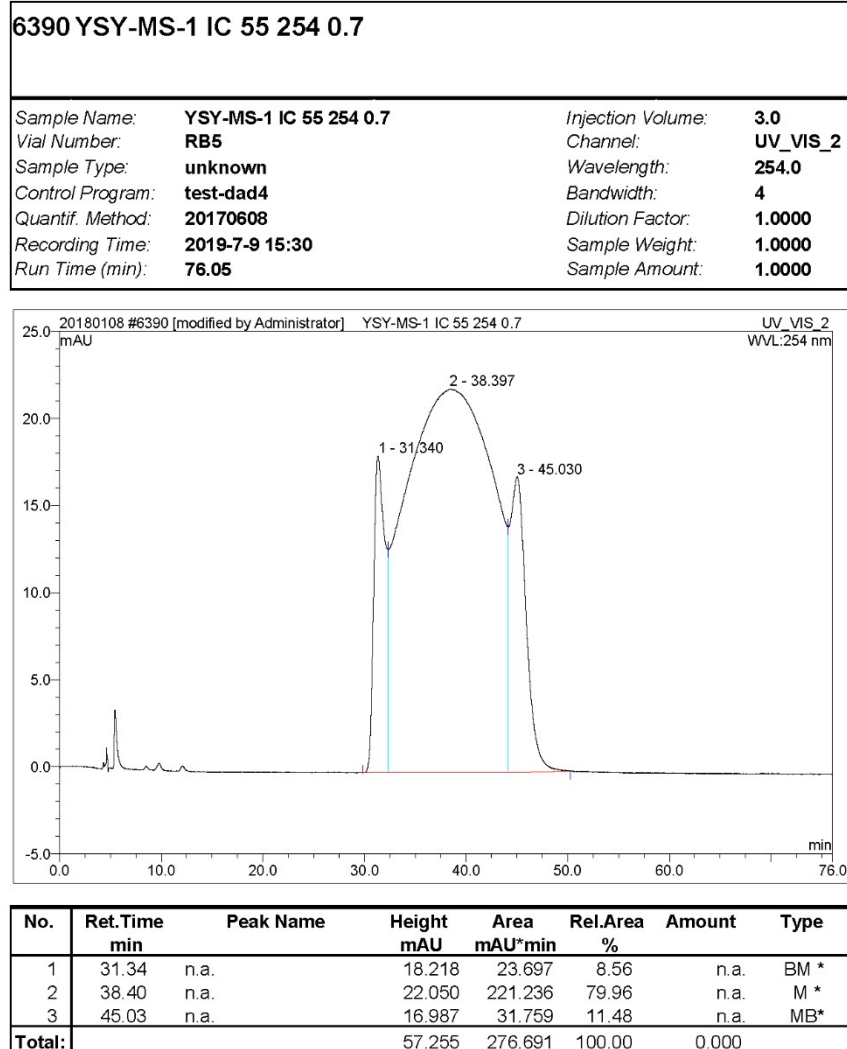
default/Integration Chromleon (c) Dionex 1996-2006  
Version 6.80 SR14 Build 4527 (238909)

**Figure S6.** HPLC profile of QPO.



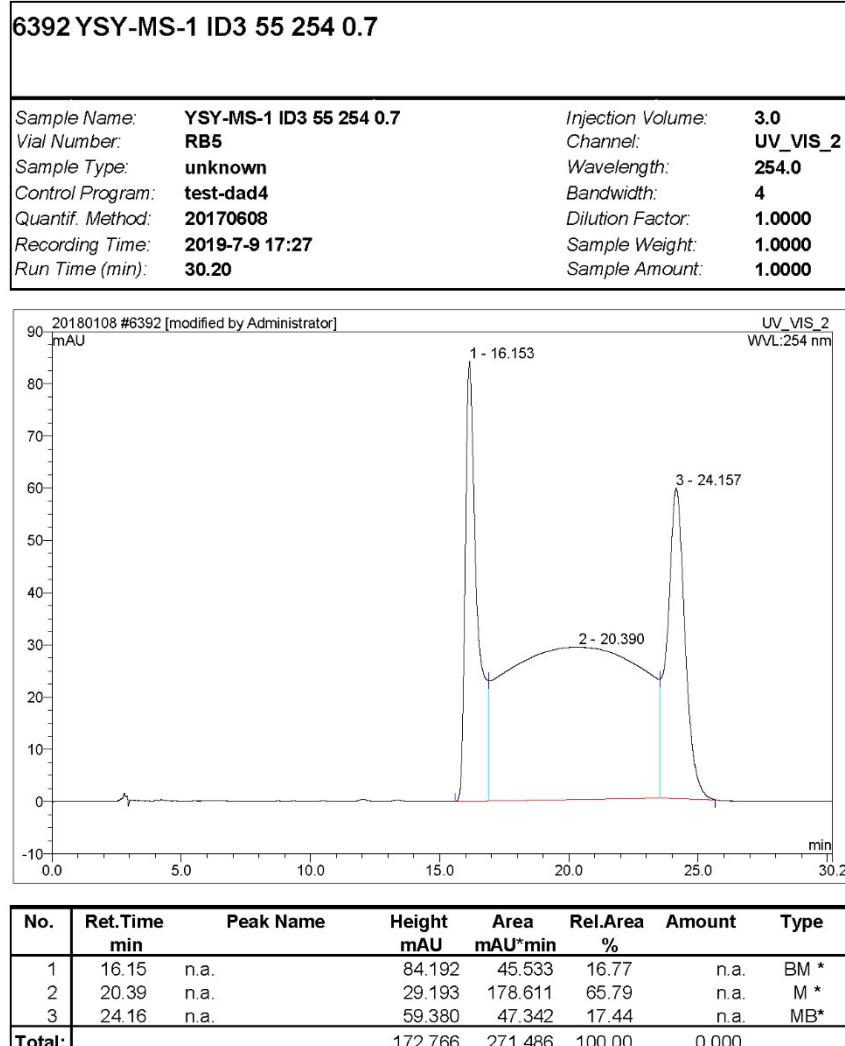
default/Integration

Chromleon (c) Dionex 1996-2006  
Version 6.80 SR14 Build 4527 (238909)**Figure S7.** HPLC profile of QPO.



default/Integration

Chromleon (c) Dionex 1996-2006  
Version 6.80 SR14 Build 4527 (238909)**Figure S8.** HPLC profile of QPO.



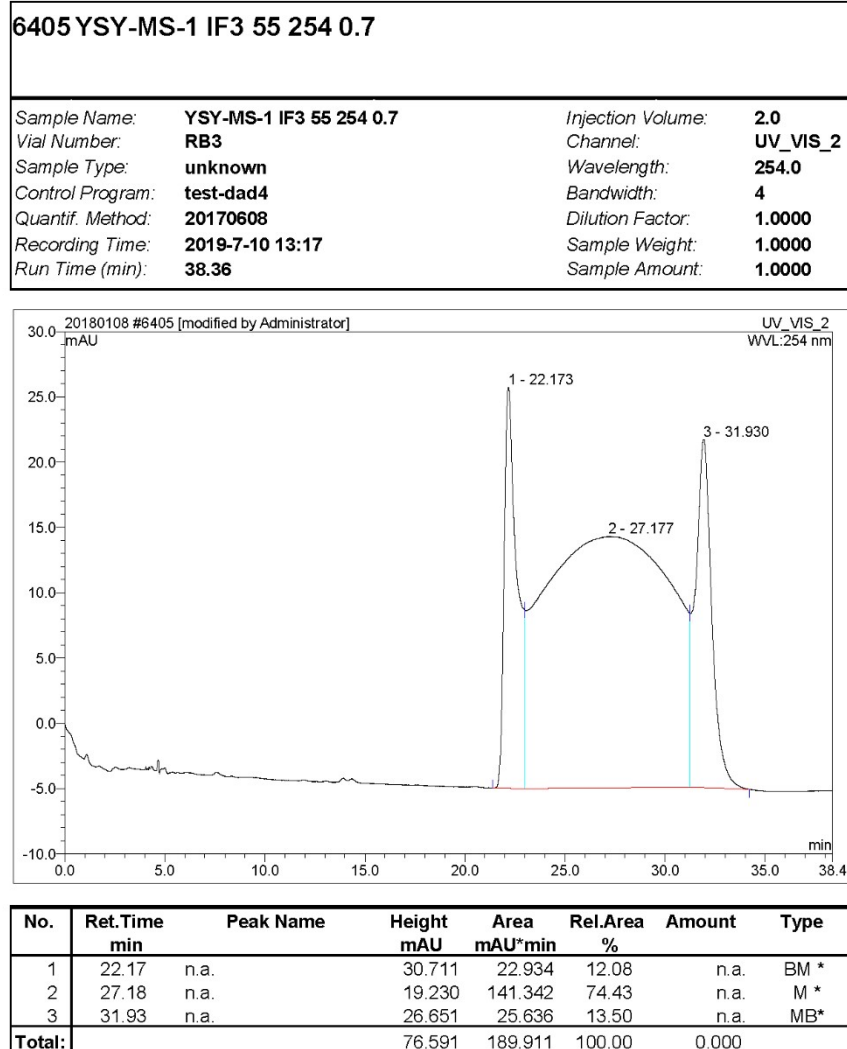
default/Integration

Chromleon (c) Dionex 1996-2006  
Version 6.80 SR14 Build 4527 (238909)**Figure S9.** HPLC profile of QPO.



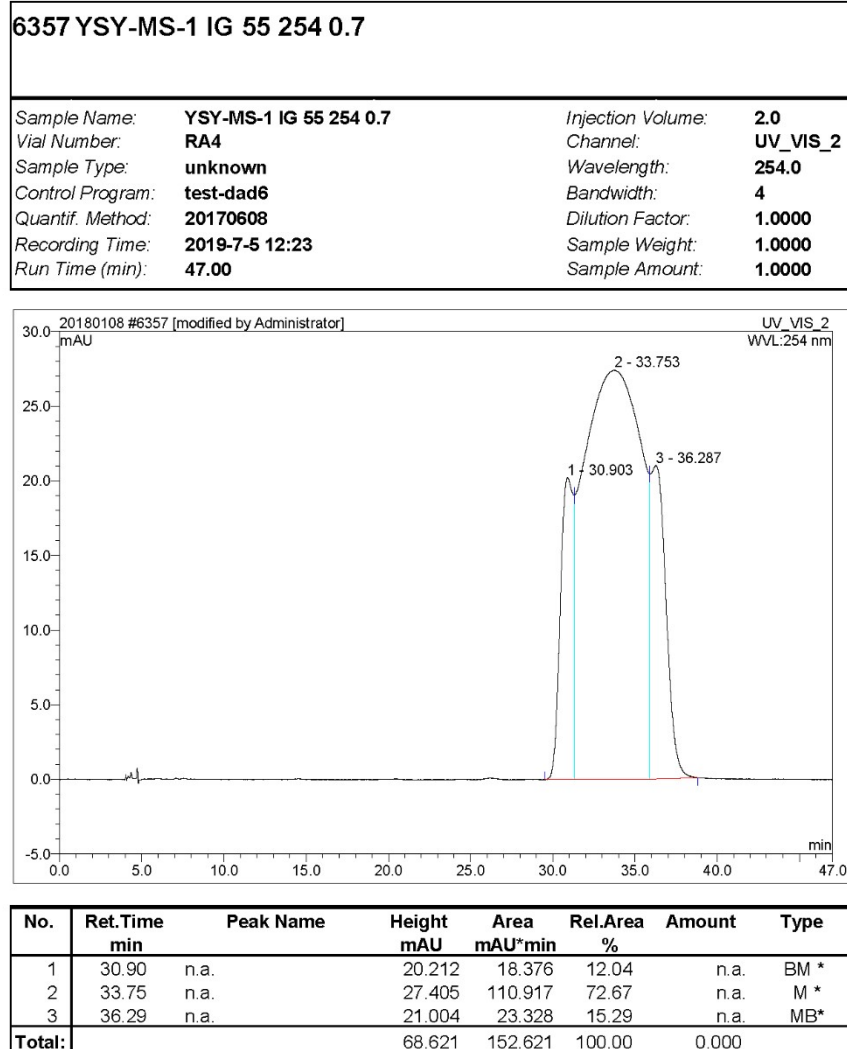
default/Integration

Chromleon (c) Dionex 1996-2006  
Version 6.80 SR14 Build 4527 (238909)**Figure S10.** HPLC profile of QPO.



default/Integration

Chromleon (c) Dionex 1996-2006  
Version 6.80 SR14 Build 4527 (238909)**Figure S11.** HPLC profile of QPO.



default/Integration

Chromleon (c) Dionex 1996-2006  
Version 6.80 SR14 Build 4527 (238909)**Figure S12.** HPLC profile of QPO.

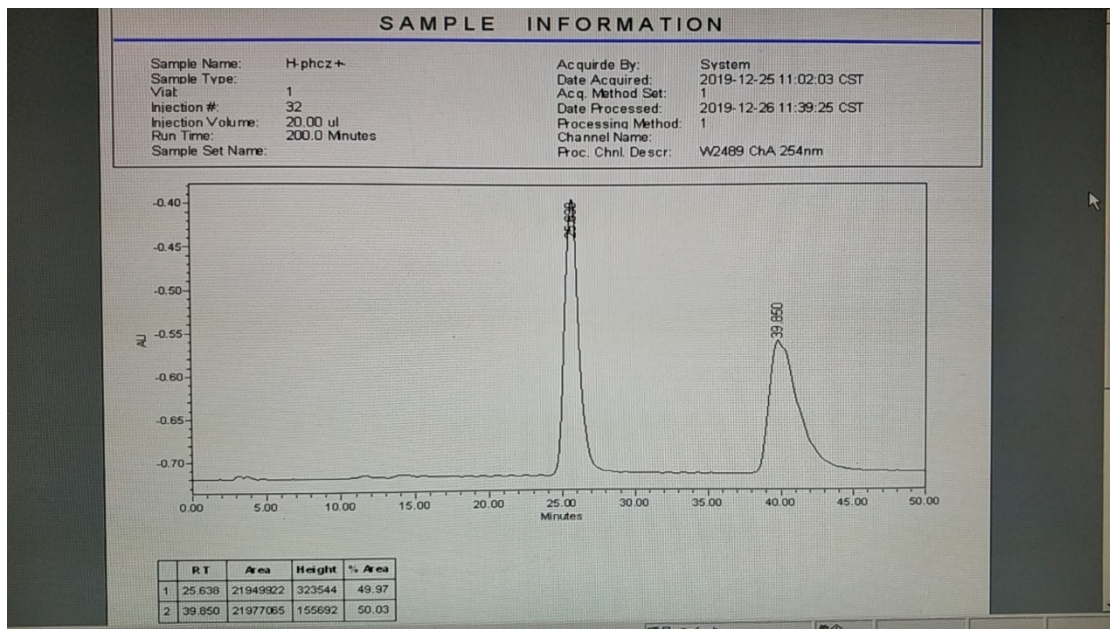


**Figure S13.** HPLC profile of QPO-PhCz.

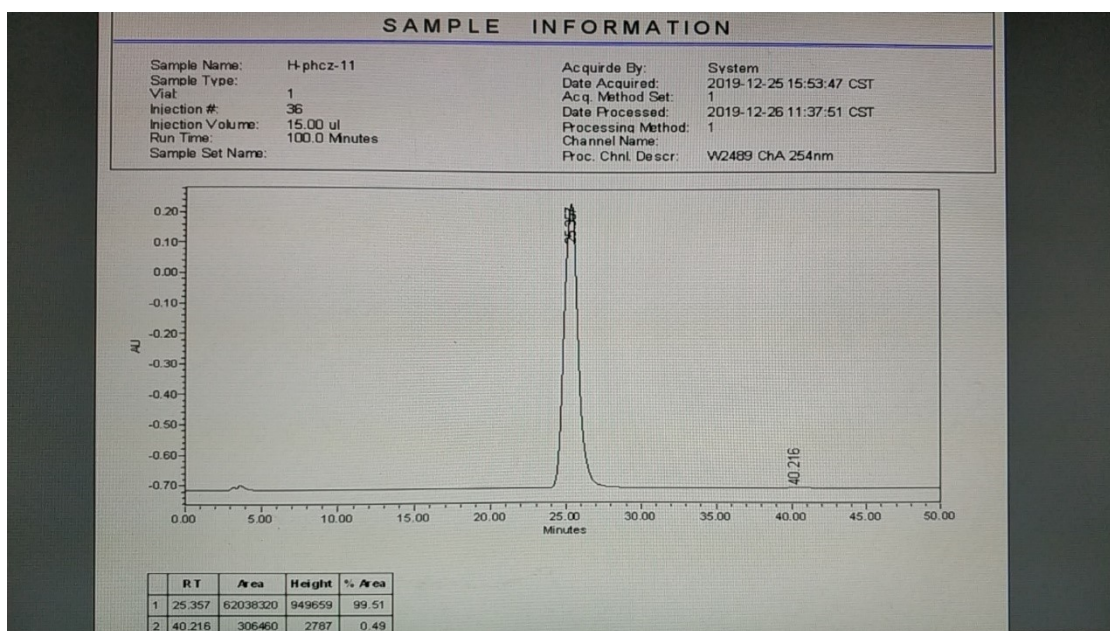


**Figure S14.** HPLC profile of (M)-QPO-PhCz.

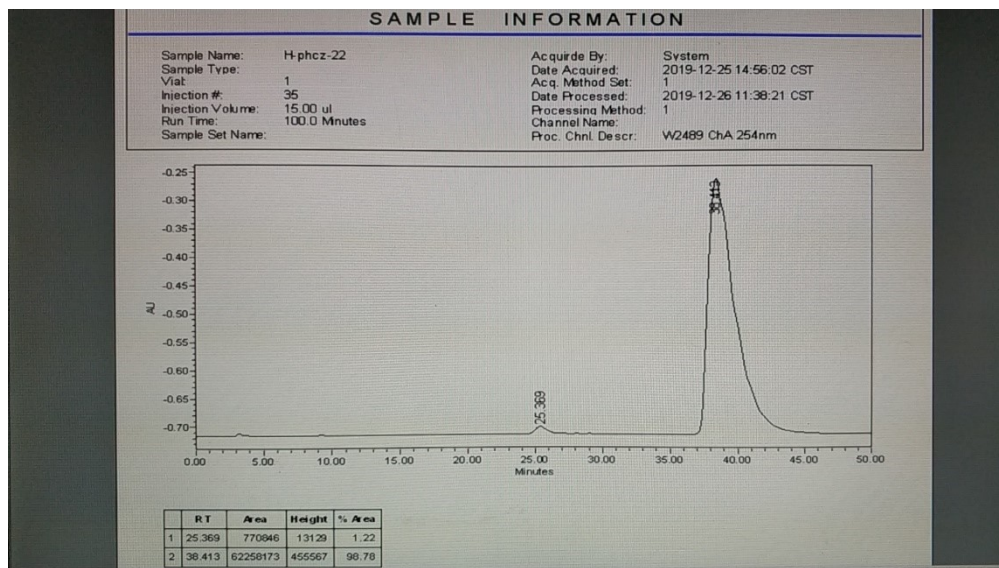


**Figure S15.** HPLC profile of (P)-QPO-PhCz.

## 2.5 Thermal properties

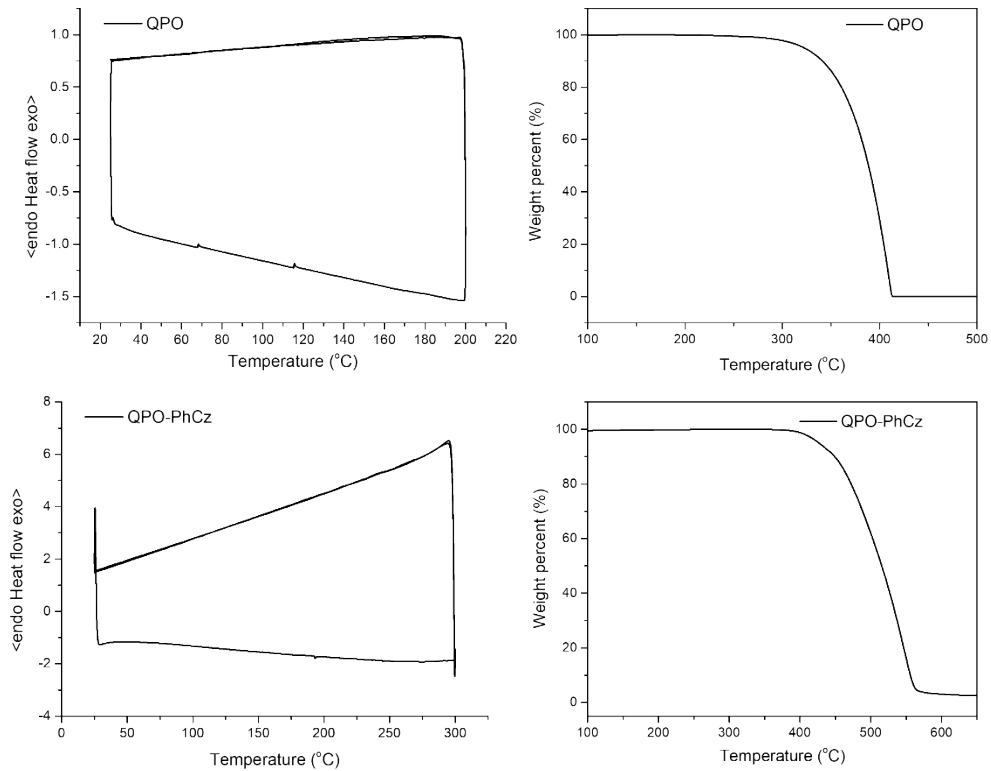


**Figure S16.** TGA/DSC curves of QPO and QPO-PhCz.

## 2.6 Electrochemical properties

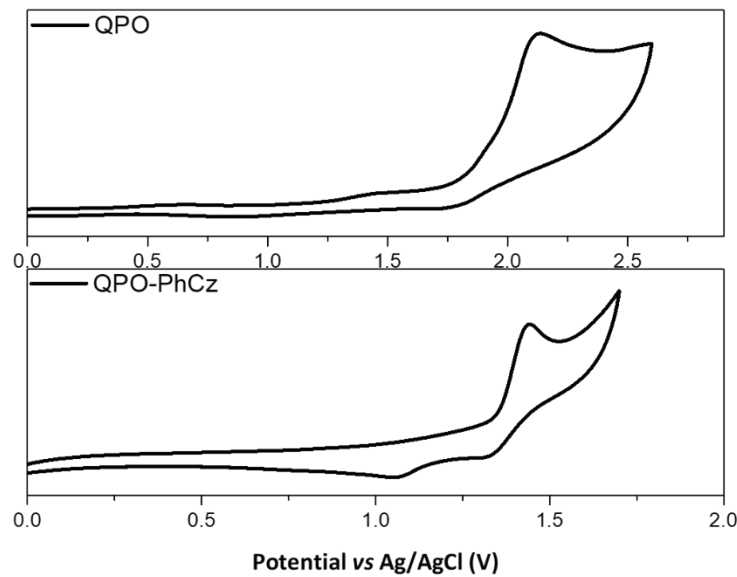


**Figure S17.** CV curves of **QPO** and **QPO-PhCz**.

## 2.7 Electroluminescence properties

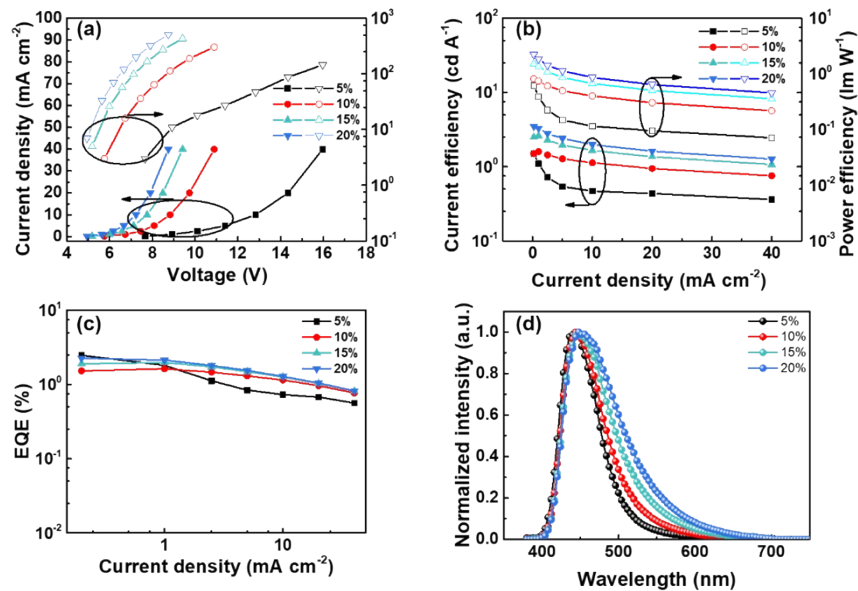


**Figure S18.** (a)  $J$ - $V$ - $L$  characteristics; (b)  $CE$ - $J$ - $PE$  characteristics; (c)  $EQE$ - $J$  characteristics and (d) EL spectra of **QPO** doped devices.

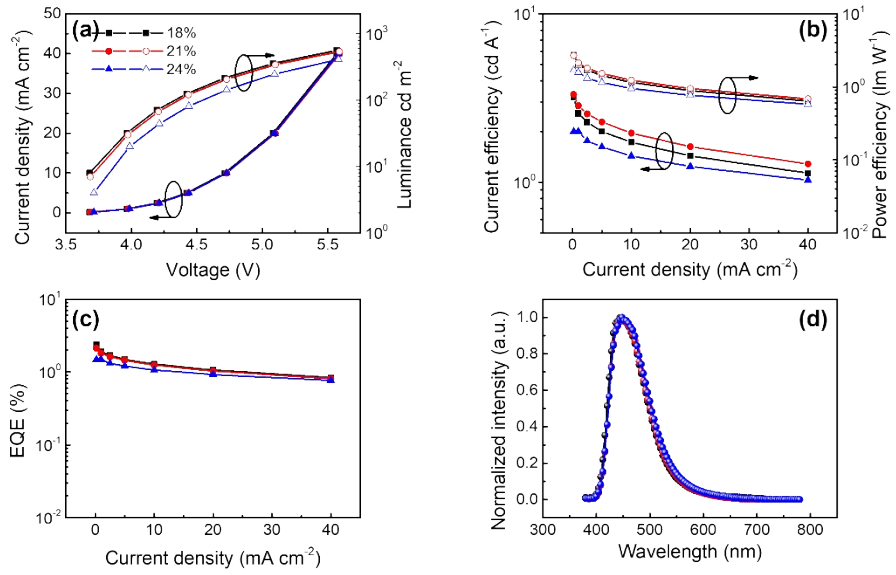


**Figure S19.** (a)  $J$ - $V$ - $L$  characteristics; (b) CE- $J$ -PE characteristics; (c) EQE- $J$  characteristics and (d) EL spectra of **QPO** doped devices.

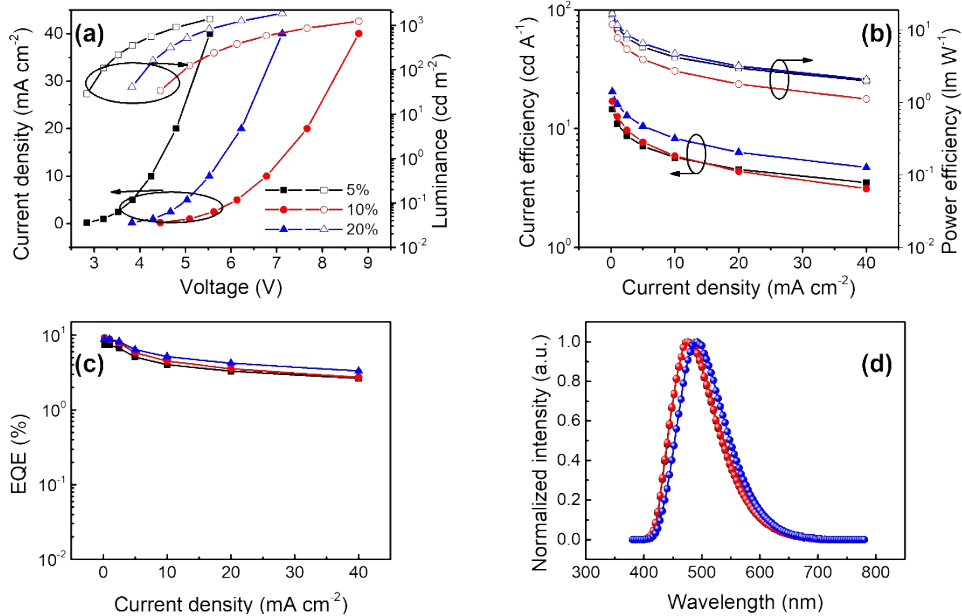


**Figure S20.** (a)  $J$ - $V$ - $L$  characteristics; (b) CE- $J$ -PE characteristics; (c) EQE- $J$  characteristics and (d) EL spectra of **QPO-PhCz** doped devices.

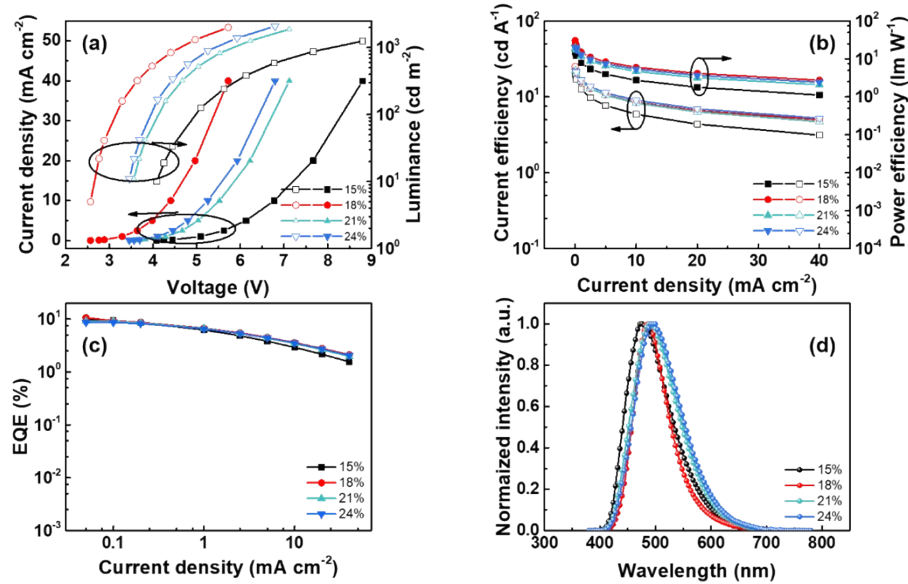


**Figure S21.** (a)  $J$ - $V$ - $L$  characteristics; (b)  $CE$ - $J$ - $PE$  characteristics; (c)  $EQE$ - $J$  characteristics and (d) EL spectra of **QPO-PhCz** doped devices.

## 2.8 Circularly polarized electroluminescence properties

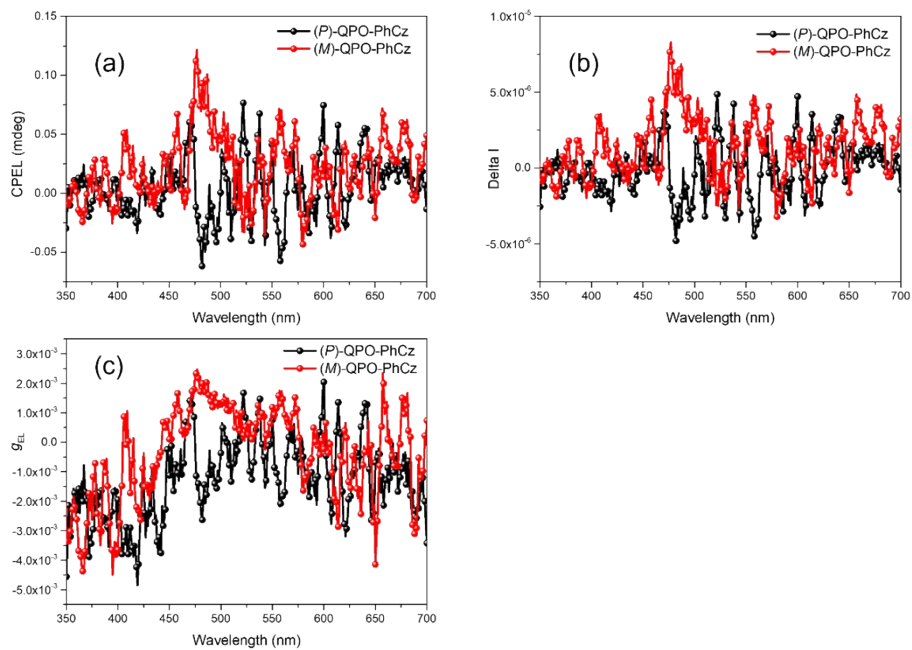


**Figure S22.** (a) Circularly polarized electroluminescence of **(P)**-QPO-PhCz/ **(M)**-QPO-PhCz; (b) CPPL spectra of **(P)**-QPO-PhCz/ **(M)**-QPO-PhCz based on  $\Delta I$ ; (c)  $g_{EL}$  curves of **(P)**-QPO-PhCz/ **(M)**-QPO-PhCz.

### 3 Supplementary Tables

#### 3.1 Crystal data and structure refinement

**Table S1** Crystal data and structure refinement for **QPO**

Empirical formula	C19H11NO3S
Formula weight	333.35
Temperature/K	100.0
Crystal system	triclinic
Space group	P-1
Unit cell dimensions	a/Å: 7.9427(4) b/Å: 8.2337(5) c/Å: 11.3541(7) α/°: 88.5360(10) β/°: 83.950(2) γ/°: 71.4370(10)
Volume/ Å <sup>3</sup>	699.96(7)
Z	2
Density/g/cm <sup>3</sup>	1.582
Absorption coefficient/mm <sup>-1</sup>	0.250
F(000)	344.0
Crystal size/mm <sup>3</sup>	0.28 × 0.15 × 0.12
Theta range for data collection/°	5.22 to 55.106
Index ranges	-10 ≤ h ≤ 8 -10 ≤ k ≤ 10 -14 ≤ l ≤ 14
Reflections collected	8610
Independent reflections	3200 [R <sub>int</sub> = 0.0400, R <sub>sigma</sub> = 0.0509]
Data/restraints/parameters	3200/0/217
Goodness-of-fit on F <sup>2</sup>	1.023
Final R indices [I>2sigma(I)]	R <sub>1</sub> = 0.0446, wR <sub>2</sub> = 0.1038
R indices (all data)	R <sub>1</sub> = 0.0615, wR <sub>2</sub> = 0.1166
Largest diff. peak and hole	0.34/-0.53
Radiation	MoKα ( $\lambda$ = 0.71073)
CCDC number	2051469

**Table S2** Crystal data and structure refinement for **QPO-PhCz**

Empirical formula	C37H22N2O3S
-------------------	-------------

Formula weight	574.62
Temperature/K	173.0
Crystal system	triclinic
Space group	P-1
Unit cell dimensions	a/Å: 9.2936(6) b/Å: 10.7266(7) c/Å: 13.7992(10) α/°: 92.415(2) β/°: 98.846(2) γ/°: 104.956(2)
Volume/ Å <sup>3</sup>	1308.38(15)
Z	2
Density/g/cm <sup>3</sup>	1.459
Absorption coefficient/mm <sup>-1</sup>	0.169
F(000)	596.0
Crystal size/mm <sup>3</sup>	0.15 × 0.11 × 0.08
Theta range for data collection/°	4.604 to 52.77
Index ranges	-11 ≤ h ≤ 11 -13 ≤ k ≤ 12 -17 ≤ l ≤ 17
Reflections collected	14836
Independent reflections	5302 [R <sub>int</sub> = 0.0474, R <sub>sigma</sub> = 0.0604]
Data/restraints/parameters	5302/0/388
Goodness-of-fit on F <sup>2</sup>	1.080
Final R indices [I>2sigma(I)]	R <sub>1</sub> = 0.0559, wR <sub>2</sub> = 0.1287
R indices (all data)	R <sub>1</sub> = 0.0873, wR <sub>2</sub> = 0.1478
Largest diff. peak and hole	0.35/-0.49
Radiation	MoKα ( $\lambda$ = 0.71073)
CCDC number	2051470

### 3.2 Electroluminescence characteristics

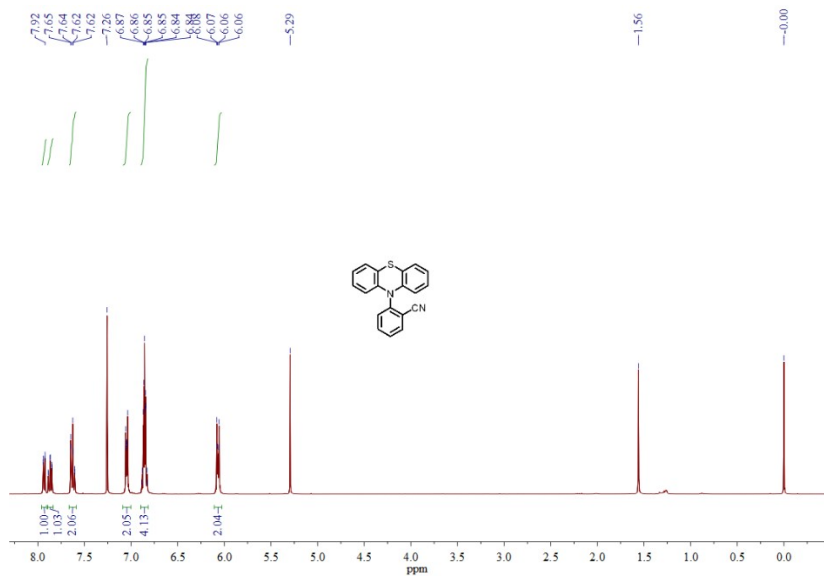
**Table S3.** Electroluminescence characteristics of the **QPO** and **QPO-PhCz** doped devices at different dopant concentrations.

Device	Dopant ratio	$\eta_{CE}^a$	$\eta_{PE}^a$	EQE <sup>a</sup> (%)	Peak wavelength <sup>b</sup> (nm)	CIE (x,y)
		(cd A <sup>-1</sup> )	(lm W <sup>-1</sup> )			
<b>QPO</b>	<b>5 wt%</b>	1.5	0.6	2.5	444	(0.16, 0.07)
	<b>10 wt%</b>	1.6	0.8	1.6	448	(0.16, 0.11)
	<b>15 wt%</b>	2.6	1.5	2.0	448	(0.16, 0.15)
	<b>18 wt%</b>	3.2	2.7	2.4	448	(0.16, 0.11)
	<b>20 wt%</b>	3.5	2.2	2.3	448	(0.17, 0.19)
	<b>21 wt%</b>	3.3	2.8	2.1	448	(0.16, 0.11)
	<b>24 wt%</b>	2.0	1.7	1.5	448	(0.16, 0.13)
<b>QPO- PhCz</b>	<b>5 wt%</b>	14.5	16.0	7.4	476	(0.18, 0.28)
	<b>10 wt%</b>	17.0	12.0	8.8	476	(0.18, 0.29)
	<b>15 wt%</b>	20.0	15.4	9.4	476	(0.18, 0.28)
	<b>18 wt%</b>	25.0	30.5	10.6	488	(0.17, 0.34)
	<b>20 wt%</b>	20.5	17.2	9.2	492	(0.20, 0.36)
	<b>21 wt%</b>	22.0	19.3	9.2	492	(0.20, 0.36)
	<b>24 wt%</b>	22.0	20.0	8.6	500	(0.21, 0.39)

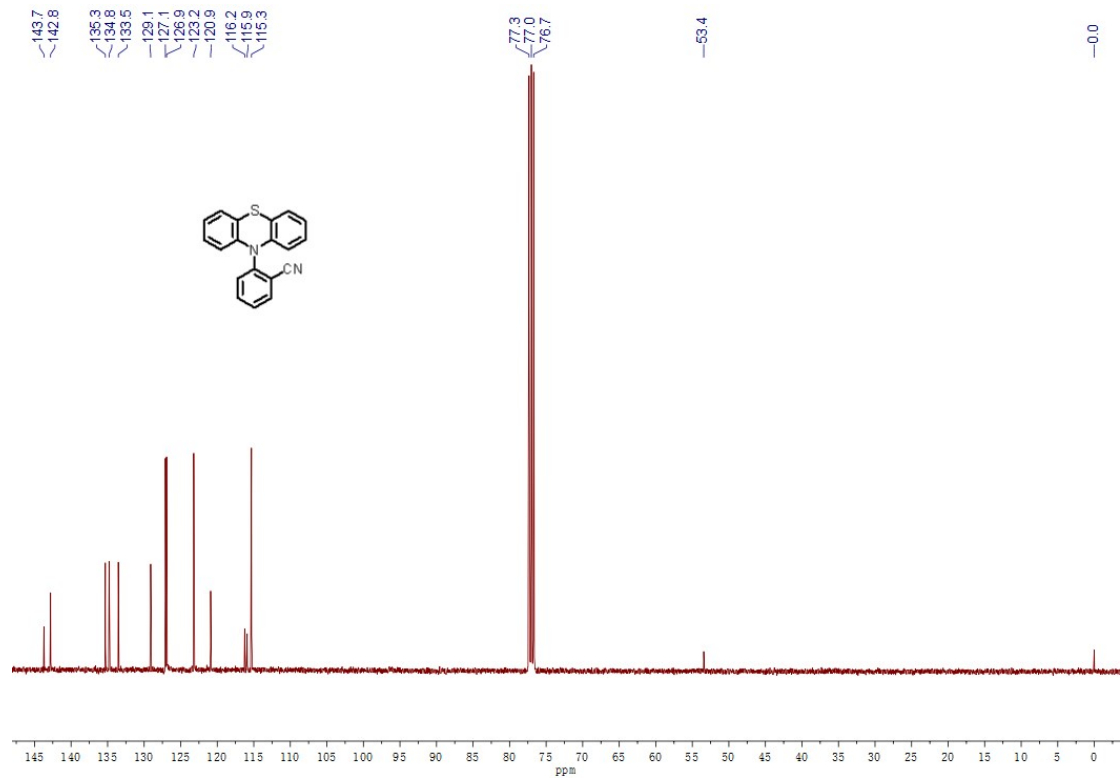
<sup>a</sup> Efficiencies in the order of the maxima. <sup>b</sup> Measured at 5 mA cm<sup>-2</sup>.

## 4 Copy of NMR Spectra and MALDI-TOF-MS Plot

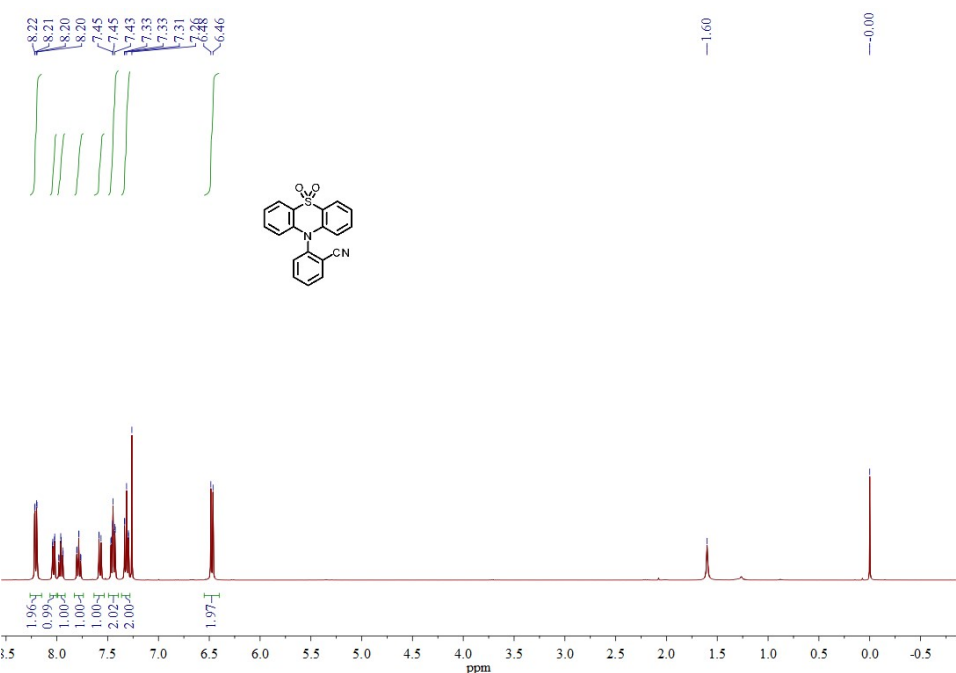
### 4.1 $^1\text{H}$ NMR plot of **2**, 400 MHz, $\text{CDCl}_3$



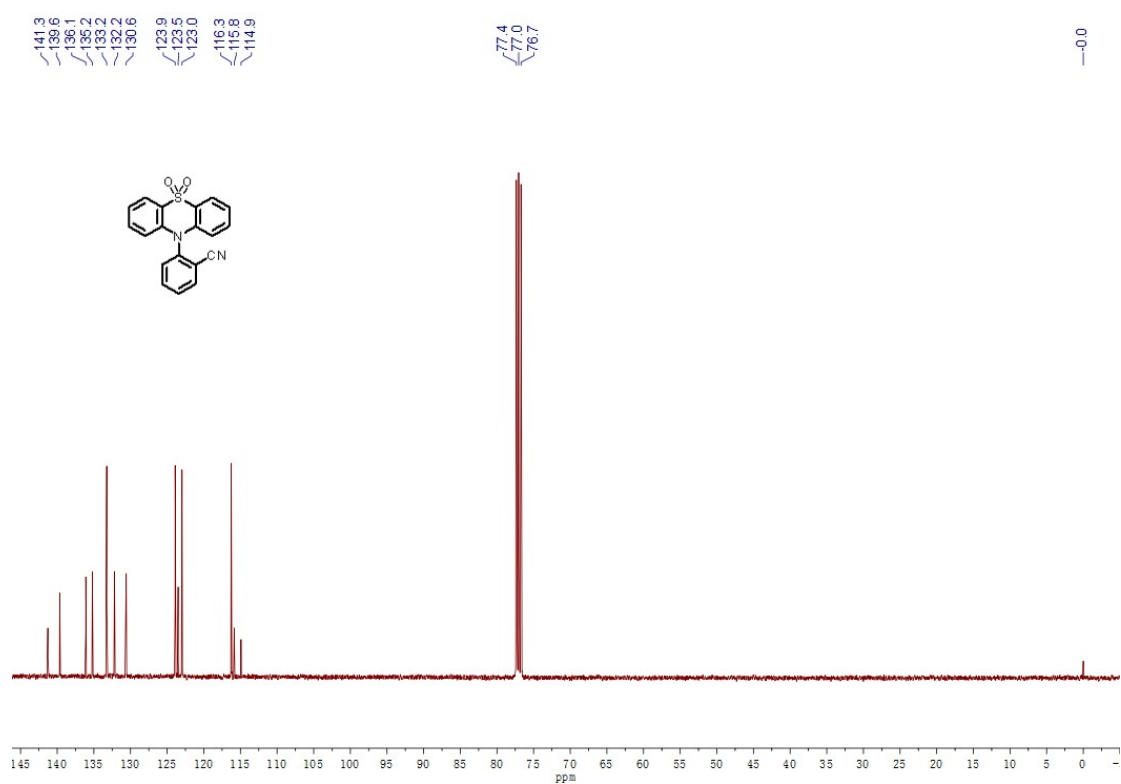
### 4.2 $^{13}\text{C}$ NMR plot of **2**, 101 MHz, $\text{CDCl}_3$



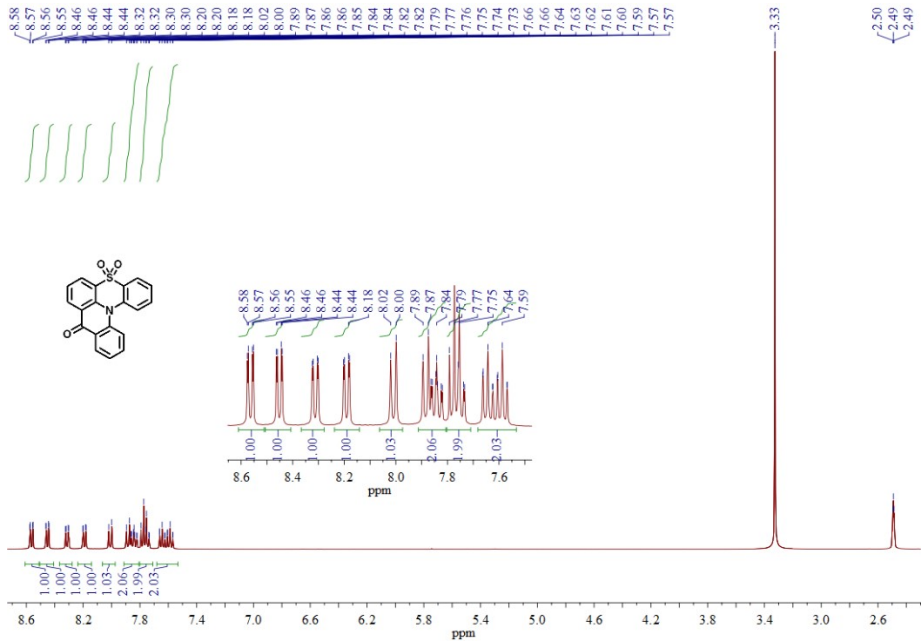
#### 4.3 $^1\text{H}$ NMR plot of **3**, 400 MHz, $\text{CDCl}_3$



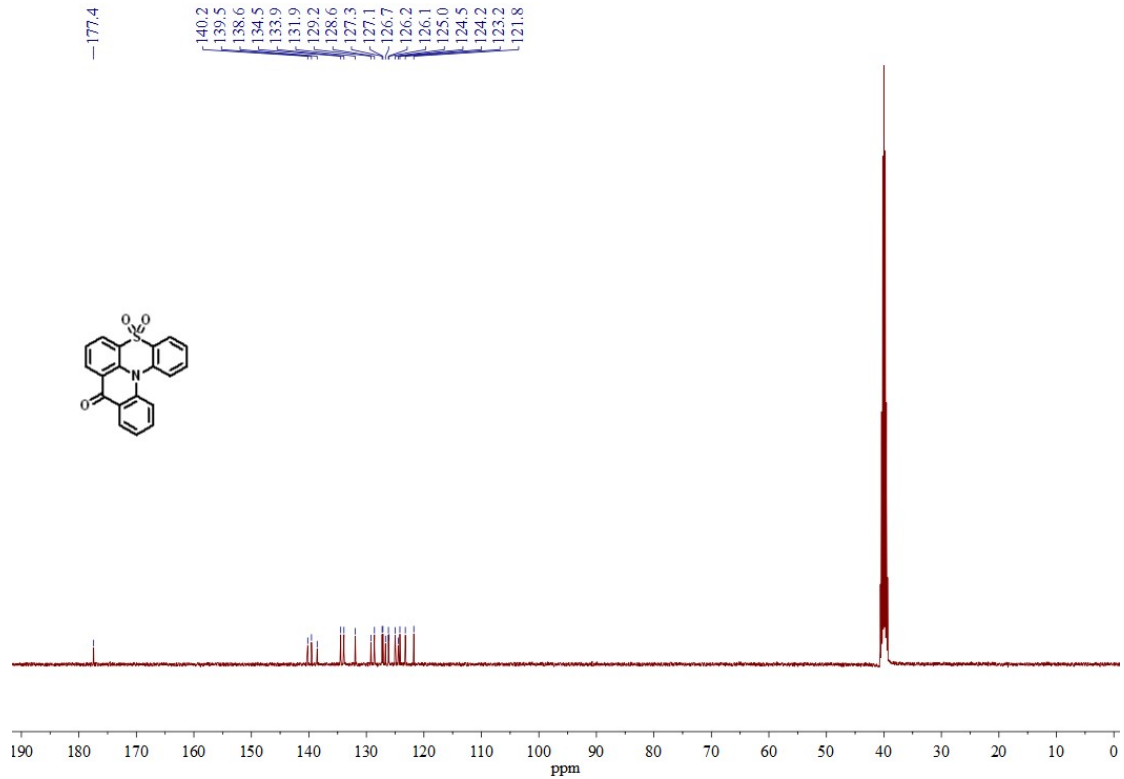
4.4  $^{13}\text{C}$  NMR plot of **3**, 101 MHz,  $\text{CDCl}_3$



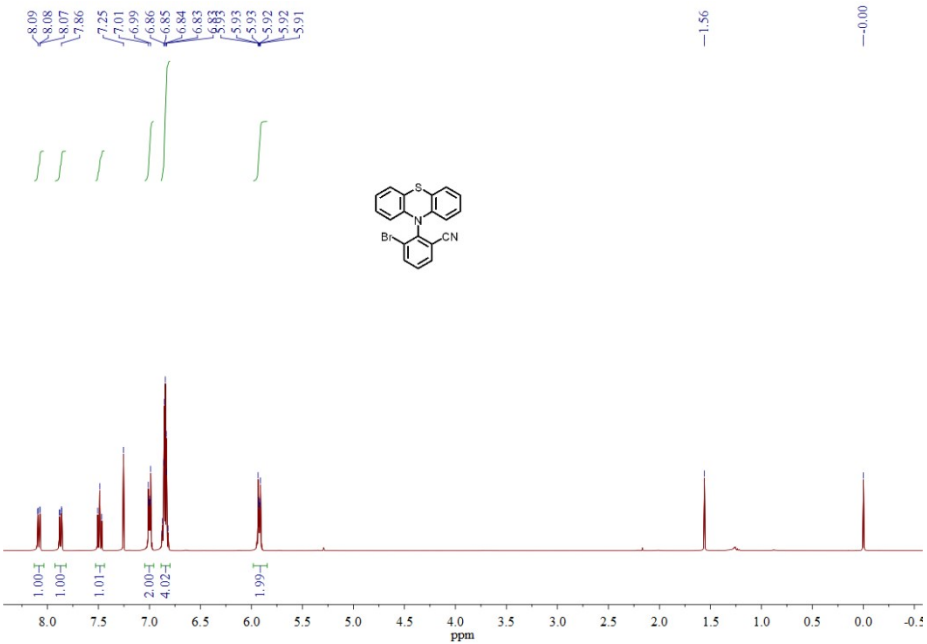
#### 4.5 $^1\text{H}$ NMR plot of QPO, 400 MHz, DMSO



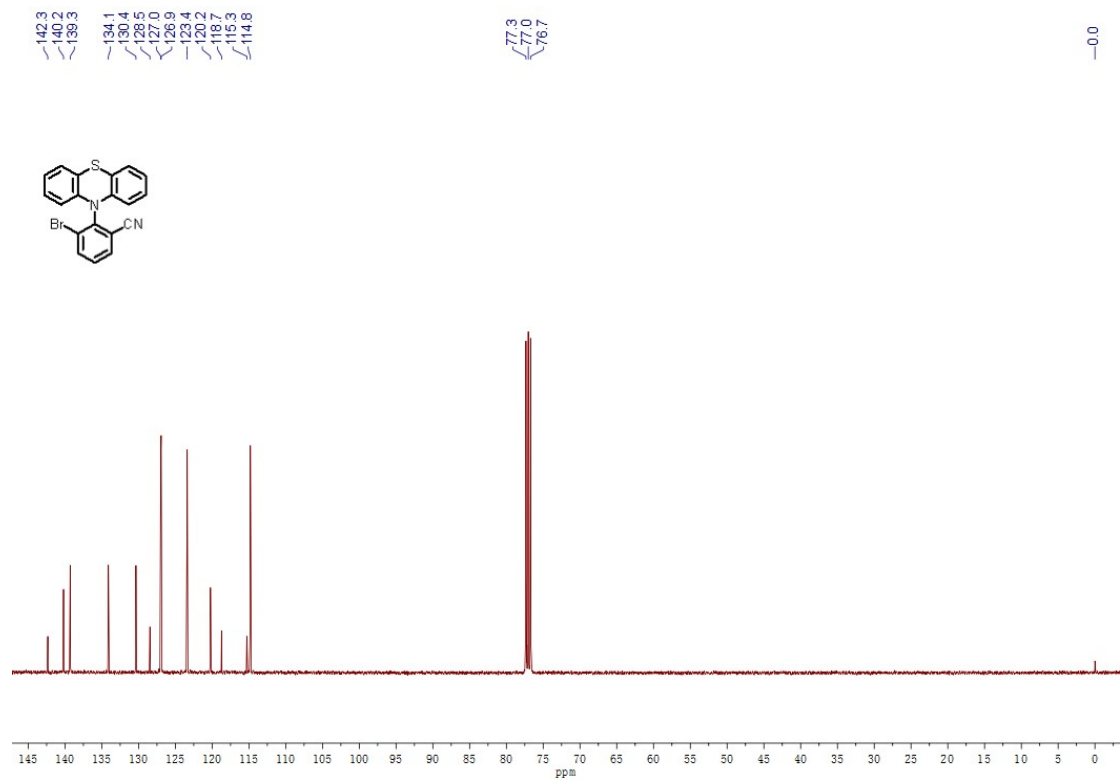
#### 4.6 $^{13}\text{C}$ NMR plot of QPO, 101 MHz, DMSO



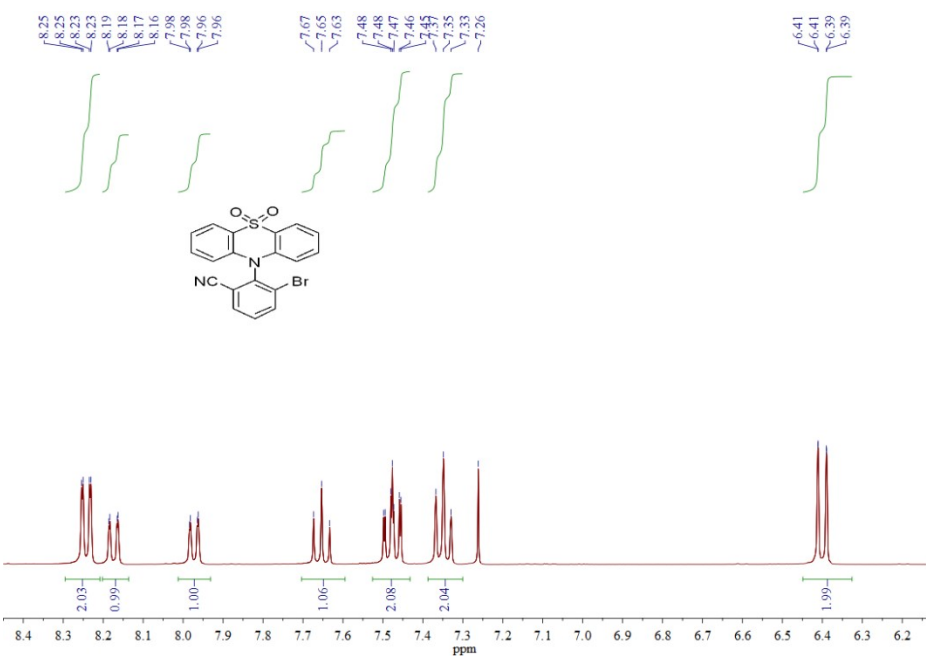
4.7  $^1\text{H}$  NMR plot of **5**, 400 MHz,  $\text{CDCl}_3$



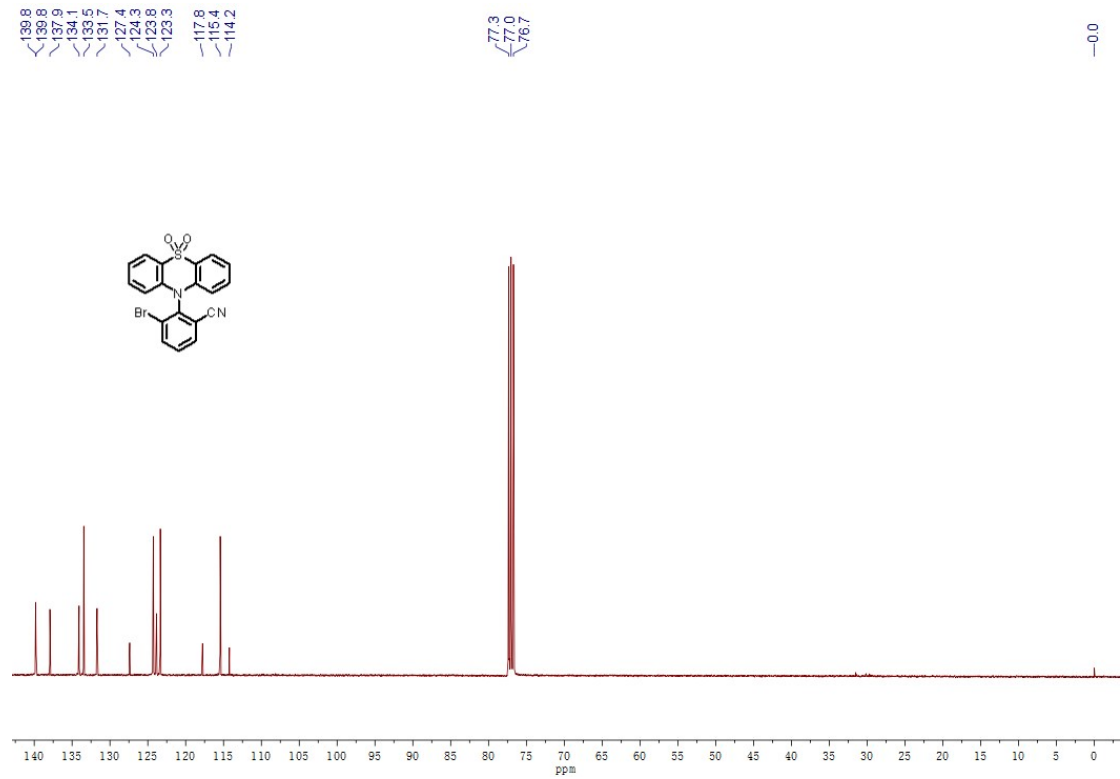
4.8  $^{13}\text{C}$  NMR plot of **5**, 101 MHz,  $\text{CDCl}_3$



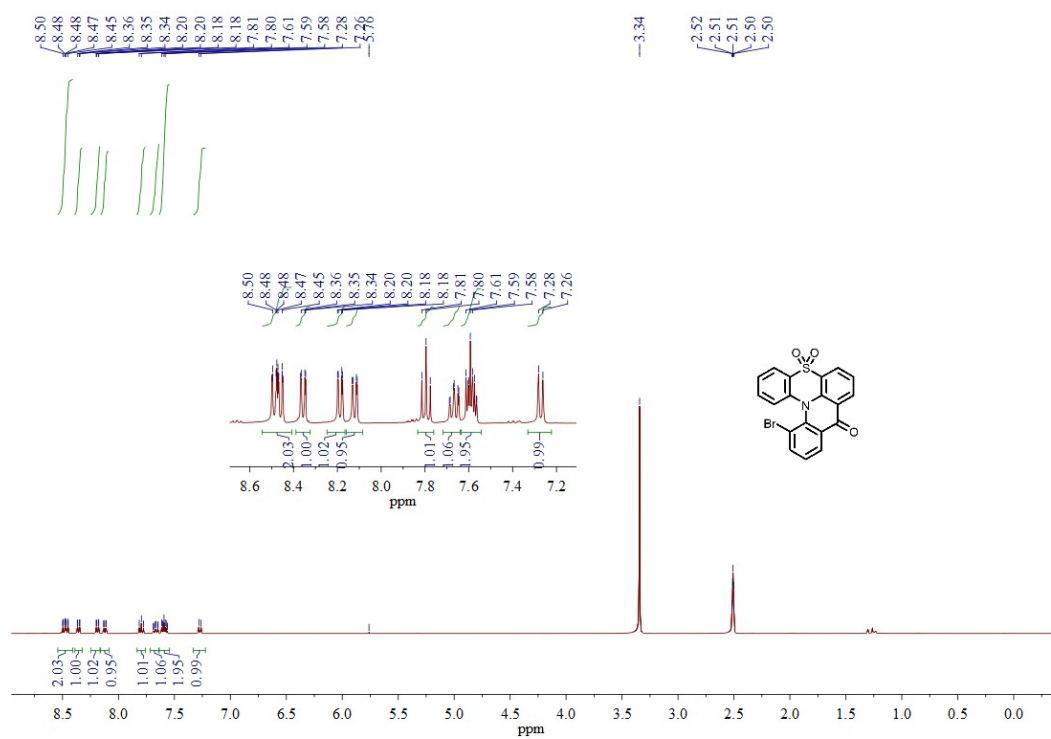
#### 4.9 $^1\text{H}$ NMR plot of **6**, 400 MHz, $\text{CDCl}_3$



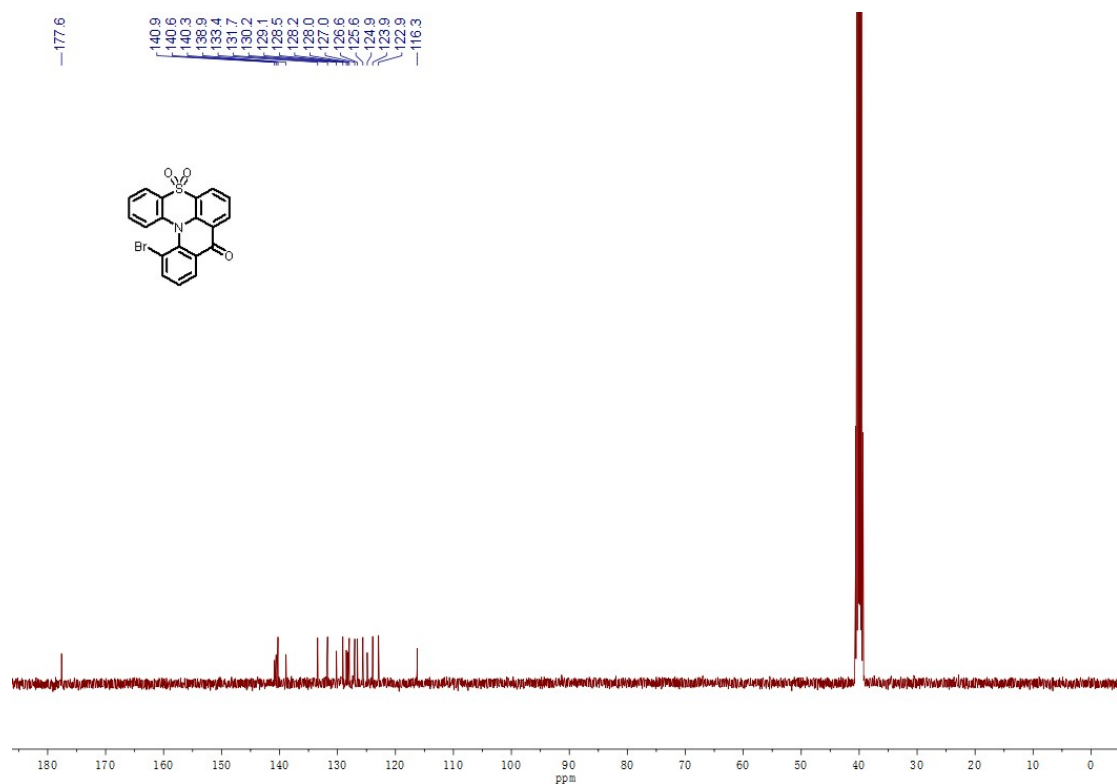
#### 4.10 $^{13}\text{C}$ NMR plot of **6**, 101 MHz, $\text{CDCl}_3$



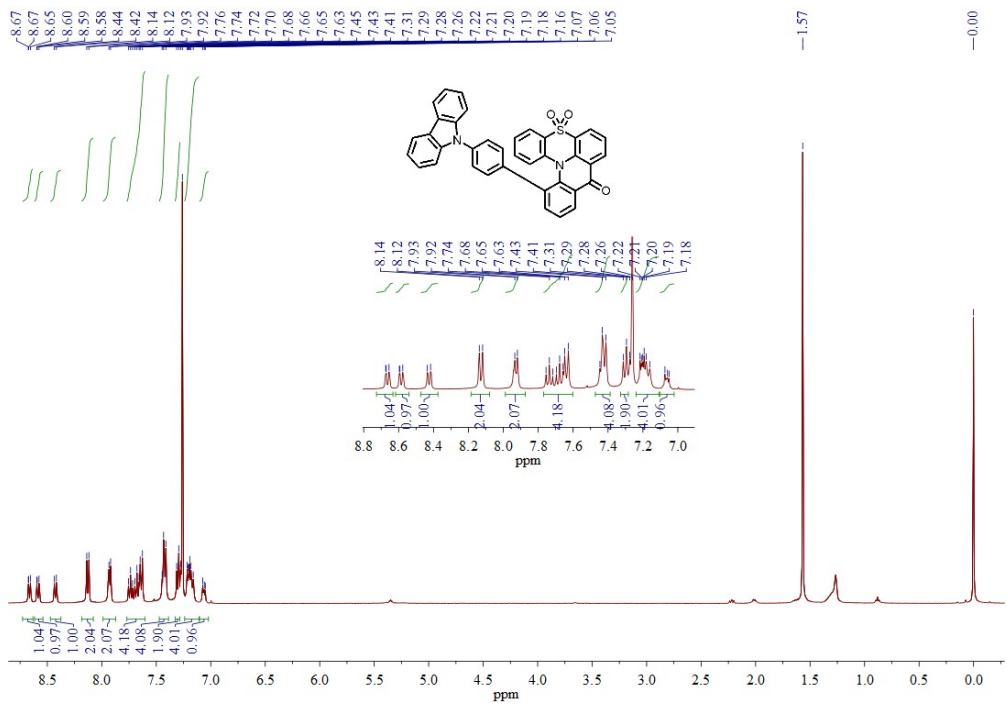
#### 4.11 $^1\text{H}$ NMR plot of QPO-Br, 400 MHz, DMSO



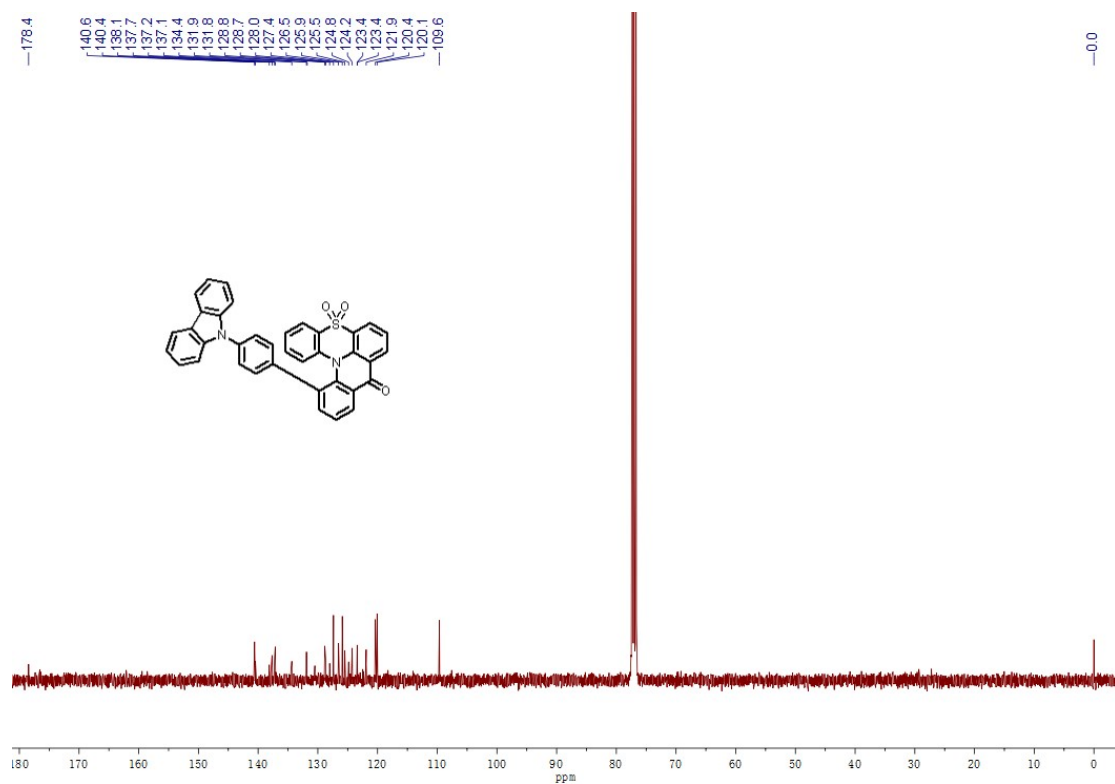
#### 4.12 $^{13}\text{C}$ NMR plot of QPO-Br, 101 MHz, DMSO



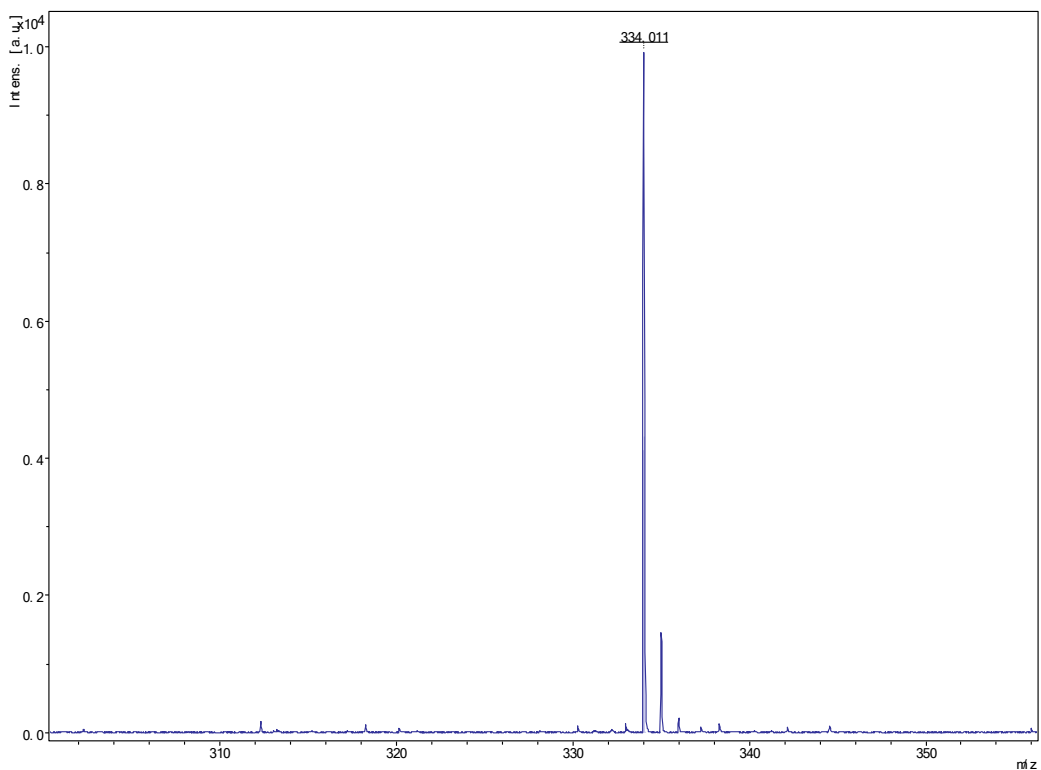
4.13  $^1\text{H}$  NMR plot of QPO-PhCz, 400 MHz,  $\text{CDCl}_3$



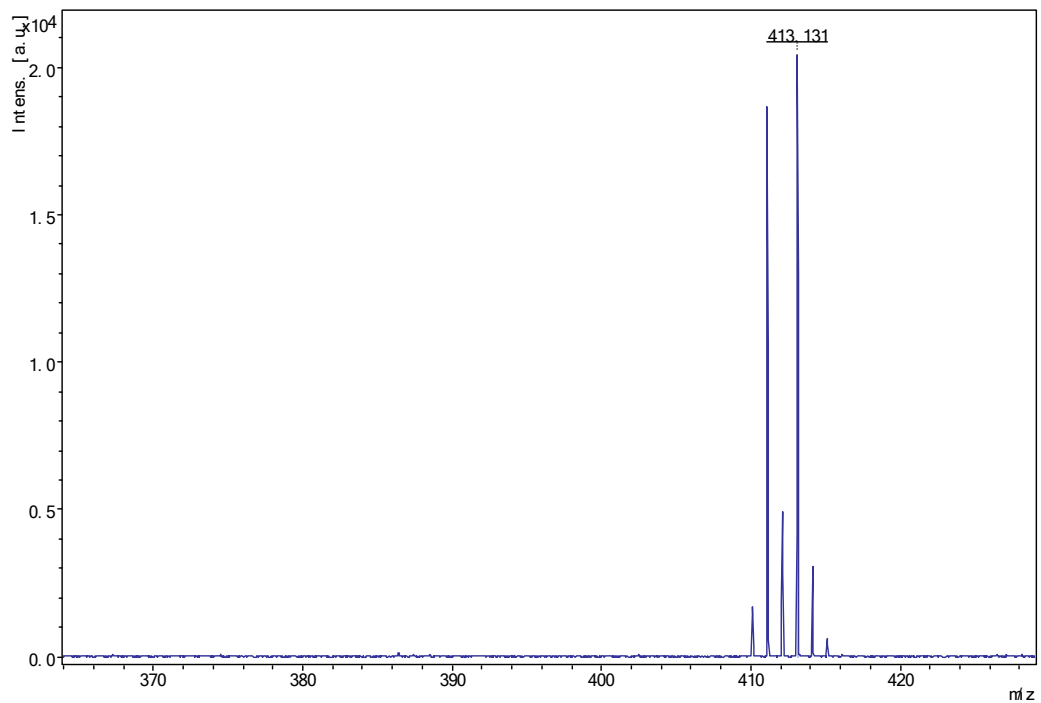
4.14  $^{13}\text{C}$  NMR plot of **QPO-PhCz**, 101 MHz,  $\text{CDCl}_3$



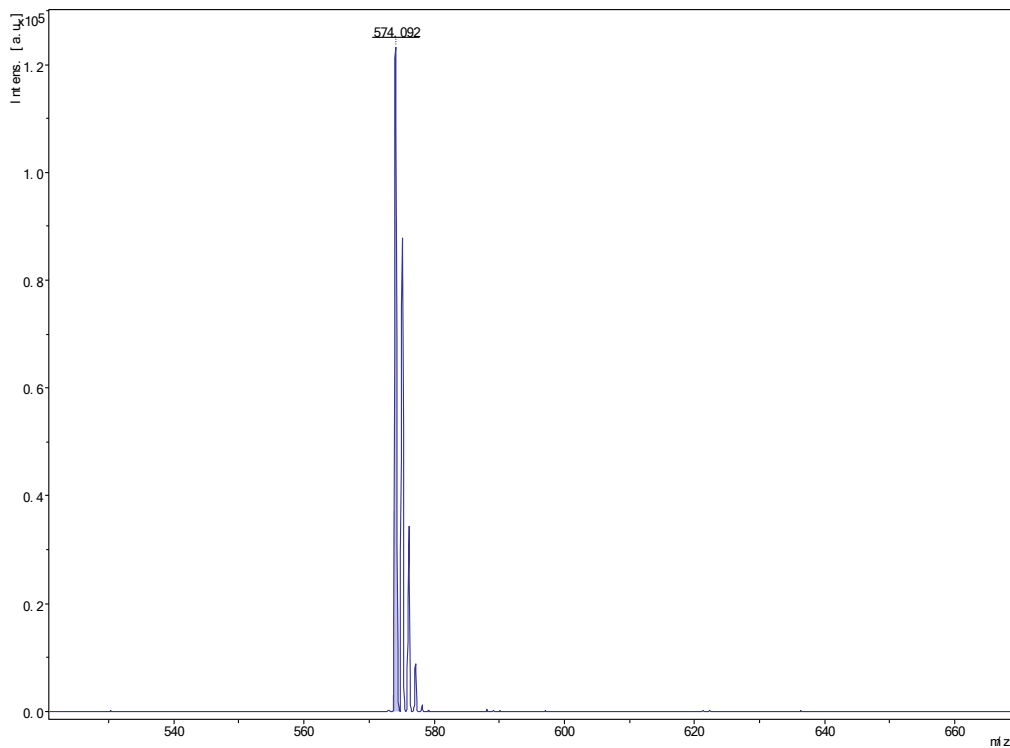
#### 4.15 MALDI-TOF-MS plot of QPO



#### 4.16 MALDI-TOF-MS plot of QPO-Br



## 4.17 MALDI-TOF-MS plot of QPO-PhCz



## 5 References

- [1] M. J. Frisch, G. W. Trucks, H. B. Schlegel, G. E. Scuseria, M. A. Robb, J. R. Cheeseman, G. Scalmani, V. Barone, B. Mennucci, G. A. Petersson, H. Nakatsuji, M. Caricato, X. Li, H. P. Hratchian, A. F. Izmaylov, J. Bloino, G. Zheng, J. L. Sonnenberg, M. Hada, M. Ehara, K. Toyota, R. Fukuda, J. Hasegawa, M. Ishida, T. Nakajima, Y. Honda, O. Kitao, H. Nakai, T. Vreven, J. A. Montgomery, Jr., J. E. Peralta, F. Ogliaro, M. Bearpark, J. J. Heyd, E. Brothers, K. N. Kudin, V. N. Staroverov, T. Keith, R. Kobayashi, J. Normand, K. Raghavachari, A. Rendell, J. C. Burant, S. S. Iyengar, J. Tomasi, M. Cossi, N. Rega, J. M. Millam, M. Klene, J. E. Knox, J. B. Cross, V. Bakken, C. Adamo, J. Jaramillo, R. Gomperts, R. E. Stratmann, O. Yazyev, A. J. Austin, R.

Cammi, C. Pomelli, J. W. Ochterski, R. L. Martin, K. Morokuma, V. G. Zakrzewski, G. A. Voth, P. Salvador, J. J. Dannenberg, S. Dapprich, A. D. Daniels, O. Farkas, J. B. Foresman, J. V. Ortiz, J. Cioslowski and D. J. Fox, Gaussian, Inc., Wallingford CT, 2013, Gaussian 09, Revision E.01.

[2] Becke, A. D. *J. Chem. Phys.* **1993**, *98*, 5648–5652.

[3] Lee, C.; Yang, W.; Parr, R. G. *Phys. Rev. B*, **1988**, *37*, 785–789.

[4] Lu, T.; Chen, F. *J. Comput. Chem.*, **2012**, *33*, 580–592.

[5] (a) Johnson, E. R.; Keinan, S.; Sanchez, P. M.; Garcia, J. C.; Cohen, A. J.; Yang, W. *J. Am. Chem. Soc.* **2010**, *132*, 6498–6506; (b) Lefebvre, C.; Rubez, G.; Khartabil, H.; Boisson, J. C.; Garcia, J. C.; Henon, E. *Phys. Chem. Chem. Phys.*, **2017**, *19*, 17928–17936.

[6] Humphrey, W.; Dalke, A.; Schulten, K. *J. Mole. Graph.*, **1996**, *14*, 33–38.